



Dynamic patterns of gene regulation I: Simple two-gene systems

Stefanie Widder^a, Josef Schicho^b, Peter Schuster^{a,c,*}

^aInstitut für Theoretische Chemie der Universität Wien, Währingerstraße 17, A-1090 Wien, Austria

^bRICAM—Johann Radon Institute for Computational and Applied Mathematics of the Austrian Academy of Sciences, Altenbergerstraße 69, A-4040 Linz, Austria

^cSanta Fe Institute, 1399 Hyde Park Road, Santa Fe, NM 87501, USA

Received 24 February 2006; received in revised form 7 January 2007; accepted 8 January 2007

Abstract

Regulation of gene activities is studied by means of computer assisted mathematical analysis of ordinary differential equations (ODEs) derived from binding equilibria and chemical reaction kinetics. Here, we present results on cross-regulation of two genes through activator and/or repressor binding. Arbitrary (differentiable) binding function can be used but systematic investigations are presented for gene–regulator complexes with integer valued Hill coefficients up to $n = 4$. The dynamics of gene regulation is derived from bifurcation patterns of the underlying systems of kinetic ODEs. In particular, we present analytical expressions for the parameter values at which one-dimensional (transcritical, saddle-node or pitchfork) and/or two-dimensional (Hopf) bifurcations occur. A classification of regulatory states is introduced, which makes use of the sign of a ‘regulatory determinant’ D (being the determinant of the block in the Jacobian matrix that contains the derivatives of the regulator binding functions): (i) systems with $D < 0$, observed, for example, if both proteins are activators or repressors, to give rise to one-dimensional bifurcations only and lead to bistability for $n \geq 2$ and (ii) systems with $D > 0$, found for combinations of activation and repression, sustain a Hopf bifurcation and undamped oscillations for $n > 2$. The influence of basal transcription activity on the bifurcation patterns is described. Binding of multiple subunits can lead to richer dynamics than pure activation or repression states if intermediates between the unbound state and the fully saturated DNA initiate transcription. Then, the regulatory determinant D can adopt both signs, plus and minus.

© 2007 Elsevier Ltd. All rights reserved.

Keywords: Basal transcription; Bifurcation analysis; Cooperative binding; Gene regulation; Hill coefficient; Hopf bifurcation

1. Introduction

Theoretical work on gene regulation goes back to the 1960s (Monod et al., 1963) soon after the first repressor protein had been discovered (Jacob and Monod, 1961). A little later the first paper on oscillatory states in gene regulation was published (Goodwin, 1965). The interest in gene regulation and its mathematical analysis never ceased (Tiwari et al., 1974; Tyson and Othmer, 1978; Smith, 1987) and saw a great variety of different attempts to design models of genetic regulatory networks that can be used in systems biology for computer simulation of *gen*(etic and

met)abolic networks.¹ Most models in the literature aim at a minimalist dynamic description which, nevertheless, tries to account for the basic regulatory functions of large networks in the cell in order to provide a better understanding of cellular dynamics. A classic in general regulatory dynamics is the monograph by Thomas and D’Ari (1990). The currently used mathematical methods comprise application of Boolean logic (Thomas and Kaufman, 2001b; Savageau, 2001; Albert and Othmer, 2003), stochastic processes (Hume, 2000) and deterministic dynamic models, examples are Cherry and Adler (2000), Bindschadler and Sneyd (2001) and Kobayashi et al. (2003) and the recent elegant analysis of bistability (Craciun et al.,

*Corresponding author. Institut für Theoretische Chemie der Universität Wien, Währingerstraße 17, A-1090 Wien, Austria.
Tel.: +43 1 4277 527 43; fax: +43 1 4277 527 93.

E-mail address: pks@tbi.univie.ac.at (P. Schuster).

¹Discussion and analysis of combined genetic and metabolic networks has become so frequent and intense that we suggest to use a separate term, *genabolic networks*, for this class of complex dynamical systems.

Nomenclature**A, B, C, ...** metabolites**[A]** = a , **[B]** = b , **[C]** = c , ... concentrations (Depending on conditions the symbols express concentrations or activities.) of metabolites**G₁, G₂** genes**[G₁]** = g_1 , **[G₂]** = g_2 concentrations of genes**Q₁, Q₂** transcribed (m)RNAs**[Q₁]** = q_1 , **[Q₂]** = q_2 concentrations of RNAs**P₁, P₂** translated proteins**[P₁]** = p_1 , **[P₂]** = p_2 concentrations of proteins**G₁ · P₂** = **H₁**, **G₂ · P₁** = **H₂** gene–protein complexes**[G₁ · P₂]** = **[H₁]** = h_1 concentrations of complexes**[G₂ · P₁]** = **[H₂]** = h_2 $K_1 = \frac{[G_2][P_1]}{[H_2]} = \frac{g_2 \cdot p_1}{h_2}$ dissociation constants $K_2 = \frac{[G_1][P_2]}{[H_1]} = \frac{g_1 \cdot p_2}{h_1}$ k_1^Q, k_2^Q transcription rate constants k_1^P, k_2^P translation rate constants d_1^Q, d_2^Q RNA degradation rate constants d_1^P, d_2^P protein degradation rate constants $F_1(p_2), F_2(p_1)$ binding (rate) functions (In case basal transcription is included the functions $F_i(p_j)$ contain also kinetic coefficients (see Section 3.3).) γ_1, γ_2 coefficients for basal transcription $\vartheta_1 = \frac{k_1^Q \cdot k_1^P}{d_1^Q \cdot d_1^P}, \vartheta_2 = \frac{k_2^Q \cdot k_2^P}{d_2^Q \cdot d_2^P}$ ratios of rate constants $\phi_1 = \frac{d_1^P}{k_1^P}, \phi_2 = \frac{d_2^P}{k_2^P}$ $D(p_1, p_2)$ regulatory determinant

$$-k_1^Q k_2^Q k_1^P k_2^P \begin{vmatrix} 0 & \left(\frac{\partial F_1}{\partial p_2}\right) \\ \left(\frac{\partial F_2}{\partial p_1}\right) & 0 \end{vmatrix}$$

 $P = (p_1, p_2)$ point in protein concentration space $\bar{P}_k = (\bar{p}_1^{(k)}, \bar{p}_2^{(k)})$ stationary point (The superscripts will be dropped in cases where ambiguity can be excluded.)

2006). In vivo constructs and selection experiments (Elowitz and Leibler, 2000; Gardner et al., 2000; Guet et al., 2002; Yokobayashi et al., 2002; Thattai and Shraiman, 2003) provide insight into regulatory dynamics and better understanding of genabolic networks. Apart from diverse minimalist models (Hartwell et al., 1999), relatively few articles are concerned with the mechanistic prerequisites for the occurrence of certain dynamic features based on positive and negative feedback loops (Thomas and Kaufman, 2001a; Ferrell, 2002) like stability, bistability, periodicity or homeostasis.

The basic gene regulation scenario that underlies the calculations presented here is sketched in Fig. 1 and has been adopted from the booklet by Ptashne and Gann (2002). Two classes of molecular effectors, activators and repressors, determine the transcriptional activity of a gene, whose activity is classified according to three states: (i) ‘naked’ DNA is commonly assumed to have a low or basal transcription activity (basal state), (ii) transcription rises to the normal level when (only) the activator is bound to the regulatory region of the gene (active state) and (iii) complexes with repressor are inactive no matter whether the activator is present or not (inactive state). We consider here cyclic regulatory interaction: $1 \rightarrow 2$ and $2 \rightarrow 1$. The basal state is sometimes also characterized as ‘leaky transcription’. We shall use this notion here for a general term in the kinetic equations that describes unregulated transcription. Effectors often become active as oligomers, commonly dimers or tetramers, and therefore we shall also refer to cases where more than one molecule has to bind before regulation becomes effective. Mathematical approaches to binding equilibria that are of relevance in gene regulation have been reviewed recently (Schuster, 2005). The genetic regulatory system is completed by

introducing translation of the transcribed mRNAs into protein regulators. Both classes of molecules, mRNAs and proteins, undergo degradation through a first-order reaction. DNA, the molecular realization of genes, is assumed to be present at constant concentration. Transcription, translation and degradation are multi-step processes and follow rather involved reaction mechanisms. A carefully studied example of such a multi-step process is template-induced RNA synthesis commonly called plus–minus RNA replication (Biebricher et al., 1983; Biebricher and Eigen, 1987). However, when monomers and enzyme, the bacteriophage Q β replicase, are present in excess, the overall kinetics follow simple first-order rate laws. We shall adopt simple kinetic first-order expressions for transcription and translation here.

Following our approach gene regulatory systems can be grouped into two classes: (i) simple systems, which are characterized by cyclic regulation ($1 \rightarrow 2, 2 \rightarrow 1$) and for which a complete (computer assisted) qualitative analysis can be carried out analytically,² and (ii) complex systems for which qualitative analysis is pending because of hard computational problems or principal difficulties. In both classes the binding functions may be arbitrarily complicated provided they are differentiable. The distinction between the two classes is made in Section 3.2 by means of a function D , the so-called ‘regulatory determinant’, which is obtained as a product of only two elements of the Jacobian matrix. In particular, all cross-regulatory two-gene systems are of class (i) no matter how sophisticated the binding functions are. In a forthcoming study (Schuster

²Computer assistance in simple problems may involve computation of solutions for equations but does not require full simulations of regulatory dynamics.

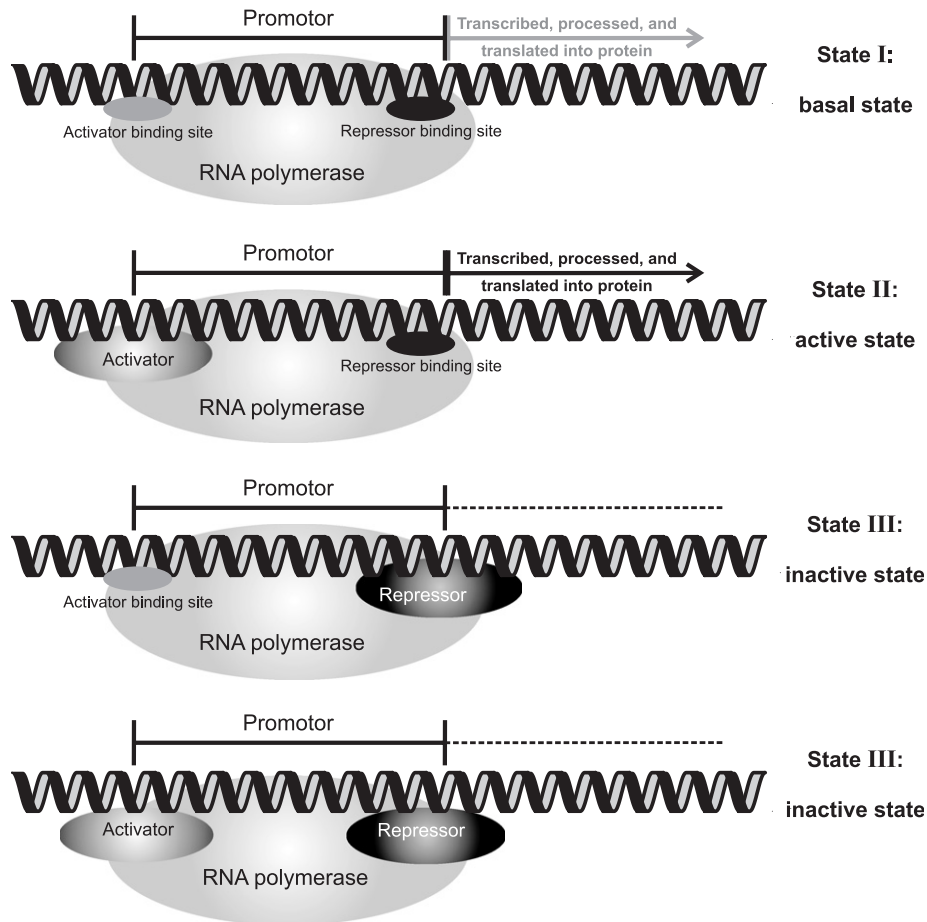


Fig. 1. Basic principle of gene regulation. The figure sketches the *regulated recruitment* mechanism of gene activity control in prokaryote cells as discovered with the *lac* genes in *Escherichia coli* (Ptashne and Gann, 2002). The gene has three states of activity, which are regulated by the presence or absence of glucose and lactose in the medium: State I, *basal state* called 'leaky transcription' occurs when both nutrients are present and it is characterized by low-level transcription; neither the activator, the CAP protein, nor the *lac*-repressor protein are bound to their sites on DNA. State II, *activated state* is induced by the absence of glucose and the presence of lactose and then CAP is bound to DNA, but *lac*-repressor protein is absent. Finally, when lactose is absent the gene is in the *inactive state* no matter whether glucose is available or not. Then, the *lac*-repressor protein is bound to DNA and transcription is blocked. The promoter region of the DNA carries specific recognition sites for the RNA polymerase in addition to the binding sites for the regulatory proteins.

et al., 2006) we shall present analogous results for cases in which the calculation is more involved as it involves more elements of the Jacobian. These systems include two-gene systems where the genes have double regulatory functions, for example, self-repression and cross-activation, and regulatory systems with more than two genes apart from those with cyclic symmetry of regulation ($1 \rightarrow 2, 2 \rightarrow 3, \dots, N \rightarrow 1$), which also fall into class (i).

Here, we present the analysis of the ordinary differential equations (ODEs) derived from chemical reaction kinetics of gene regulation under the assumption of fast binding equilibria. Only a few new results are presented in this contribution. Instead we exploit the analytical approach further than in other papers and present a new access to bifurcation analysis that allows for straightforward classification of dynamical systems for gene regulation. Qualitative analysis of the dynamical systems is performed and yields stationary points in form of the roots of high-order

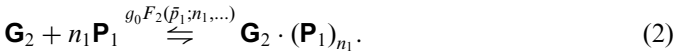
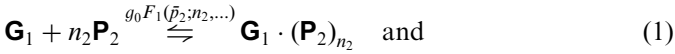
polynomials as well as simple expressions derived through differentiation of binding functions for the prediction of bifurcations and their nature (e.g. transcritical, saddle-node, pitchfork or Hopf bifurcation). Then follows a discussion of some special cases with one-step binding functions and Hill coefficients up to $n = 4$ as well as two examples of more complicated binding functions. Occasionally, we mention continuations of the phase portraits of ODEs into octants with negative concentrations when they are useful for an understanding of the regulatory dynamics.

2. Kinetic equations

2.1. Binding equilibria

The DNA is assumed to carry two genes, \mathbf{G}_1 and \mathbf{G}_2 , which have binding sites for effectors, activators and/or repressors in the promoter region. Binding of the proteins

is assumed to occur fast compared to transcription and translation, and accordingly the equilibrium assumption is valid. The binary interaction is restricted to cross-regulation of the two genes: the translation product of gene \mathbf{G}_1 controls the activity of gene \mathbf{G}_2 and vice versa. In other words, the activity of gene \mathbf{G}_1 is a function F_1 of the equilibrium concentration of protein \mathbf{P}_2 , denoted by \bar{p}_2 , and gene \mathbf{G}_2 is likewise controlled by \mathbf{P}_1 as expressed by F_2 and \bar{p}_1 , respectively. Since the number of DNA molecules is assumed to be constant, both genes are present at the same total concentrations: $(g_1)_0 = (g_2)_0 = g_0$. In general, the equilibrium is of the form



For the simplest possible case, binding equilibria of monomers, $n_1 = n_2 = 1$, and mass action we obtain³



With $K_1 = [\mathbf{G}_1][\mathbf{P}_2]/[\mathbf{G}_1 \cdot \mathbf{P}_2]$ and $K_2 = [\mathbf{G}_2][\mathbf{P}_1]/[\mathbf{G}_2 \cdot \mathbf{P}_1]$ the equilibrium concentration of the gene–protein complex is expressed by

$$[\mathbf{G}_1 \cdot \mathbf{P}_2] = \bar{c}_1 = g_0 \cdot \frac{\bar{p}_2}{K_2 + \bar{p}_2} \approx g_0 \cdot \frac{(\bar{p}_2)_0}{K_2 + (\bar{p}_2)_0},$$

$$[\mathbf{G}_2 \cdot \mathbf{P}_1] = \bar{c}_2 = g_0 \cdot \frac{\bar{p}_1}{K_1 + \bar{p}_1} \approx g_0 \cdot \frac{(\bar{p}_1)_0}{K_1 + (\bar{p}_1)_0},$$

where we approximate the equilibrium protein concentrations by the total concentrations, $\bar{p}_1 \approx (p_1)_0$ and $\bar{p}_2 \approx (p_2)_0$, assuming that the numbers of genes are much smaller than the numbers of effector molecules. In order to formulate cross-regulation of two genes in versatile form we generalize the dimensionless binding functions, F_j , $j = 1, 2$, to cooperative interactions with arbitrary exponents n :

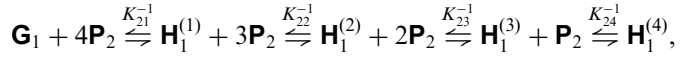
$$\text{Gene '1' } \begin{cases} F_1^{(\text{act})}(p_2; K_2, n) = \frac{p_2^n}{K_2 + p_2^n} & \text{activation,} \\ F_1^{(\text{rep})}(p_2; K_2, n) = \frac{K_2}{K_2 + p_2^n} & \text{repression,} \end{cases} \quad \text{Gene '2' } \begin{cases} F_2^{(\text{act})}(p_1; K_1, n) = \frac{p_1^n}{K_1 + p_1^n} & \text{activation,} \\ F_2^{(\text{rep})}(p_1; K_1, n) = \frac{K_1}{K_1 + p_1^n} & \text{repression.} \end{cases} \quad (5)$$

Here, ‘rep’ and ‘act’ stand for repression and activation, respectively, where either the free gene, \mathbf{G}_j , or the complex, $\mathbf{G}_j \mathbf{P}_i$, initiates transcription. The exponent n , in particular when determined experimentally, is called the Hill coefficient. (See Hill, 1910; Cantor and Schimmel, 1980,

³It will turn out that the usage of dissociation rather than binding constants is of advantage and therefore we define $K = [\mathbf{G}][\mathbf{P}]/[\mathbf{G} \cdot \mathbf{P}]$.

p. 864ff.) The Hill coefficient n is related to the molecular binding mechanism. In simple cases n is the number of protein monomers required for saturation of binding to the DNA.

More than one parameter will be required for describing binding equilibria that involve more than one protein subunit. To illustrate by means of an example, we consider consecutive binding of four ligands \mathbf{P}_2 to gene \mathbf{G}_1 ,



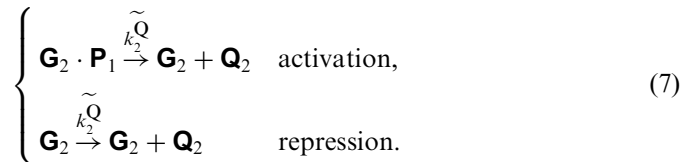
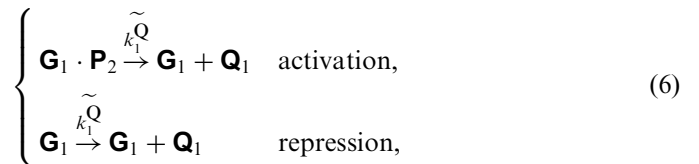
where $\mathbf{H}_1^{(k)} = \mathbf{G}_1 \cdot (\mathbf{P}_2)_k$, the complex formed by the gene with k protein monomers. If the only complex that is active in transcription were $\mathbf{H}_1^{(4)}$ the binding function would adopt the form⁴

$$F_1^{(\text{act})}(p_2; K_{21}, \dots, K_{24}) = \frac{p_2^4}{K_{21}K_{22}K_{23}K_{24} + K_{22}K_{23}K_{24}p_2 + K_{23}K_{24}p_2^2 + K_{24}p_2^3 + p_2^4}.$$

Examples of other binding functions will be discussed together with the results derived for the individual systems.

2.2. Reaction kinetics

The transcription reactions come in two variants, an activating mode (corresponding to state II of Fig. 1) and a repressing mode (corresponding to state III of Fig. 1). The basal state (state I) can be included in the activating or the repressing mode as we shall see later. The kinetic reaction mechanism for transcription then has the following form:



In case of activation, the regulator–gene complexes are transcribed, whereas the complexes are inactive in repression and then transcription is mediated by the free genes.

In contrast to DNA, the transcription products, the mRNAs \mathbf{Q}_1 and \mathbf{Q}_2 , as well as the regulators, the proteins \mathbf{P}_1 and \mathbf{P}_2 , have only finite lifetime because of decay reactions. For translation of mRNAs and for degradation

⁴The equilibrium constants applied are *macroscopic dissociation constants*. For equivalent microscopic constants the individual terms in the denominator receive the binomial coefficients, (1, 4, 6, 4, 1), as factors (Cantor and Schimmel, 1980).

of mRNAs as well as proteins we find

$$\mathbf{Q}_i \xrightarrow{k_i^P} \mathbf{Q}_i + \mathbf{P}_i, \quad i = 1, 2 \quad \text{translation,} \quad (8)$$

$$\mathbf{Q}_i \xrightarrow{d_i^Q} 0, \quad i = 1, 2 \quad \text{degradation and} \quad (9)$$

$$\mathbf{P}_i \xrightarrow{d_i^P} 0, \quad i = 1, 2 \quad \text{degradation.} \quad (10)$$

Translation and degradation reactions are modelled as simple single step processes. The approximation for translation is well justified in case of excess monomers, ribosomes and other translation factors (as mentioned in the Introduction). Simple degradation reactions are always of first order. Since the total concentration of the genes is constant and since we shall apply only binding functions that are proportional to g_0 , we can absorb the DNA concentration in the rate constant for transcription: $k_i^Q = k_i^Q g_0$. As a consequence the rate parameters have different dimensions $[k_i^Q] = [m \times t^{-1}]$ and $[k_i^P] = [d_i^Q] = [d_i^P] = [t^{-1}]$ where m stands for ‘molar’ and t stands for ‘time’. These substitutions are advantageous in a second aspect too: the regulatory functions are dimensionless, no matter whether we are using simple hyperbolic or higher order binding equilibria.

Now, we are in a position to write down the kinetic differential equations for all four molecular species, \mathbf{Q}_1 , \mathbf{Q}_2 , \mathbf{P}_1 and \mathbf{P}_2 , derived from two genes:

$$\frac{dq_i}{dt} = \dot{q}_i = k_i^Q F_i(p_j) - d_i^Q q_i, \quad i = 1, 2, \quad j = 2, 1 \quad \text{and} \quad (11)$$

$$\frac{dp_i}{dt} = \dot{p}_i = k_i^P q_i - d_i^P p_i, \quad i = 1, 2. \quad (12)$$

Accordingly, the dynamical system contains eight kinetic parameters and two binding functions. Except for the binding functions $F_i(p_j)$ the system is linear. This property will be important for analyzing the Jacobian matrix and determining the stability of stationary points.

3. Qualitative analysis

3.1. Determination of stationary points

In order to derive equations for the stationary or fixed points of the dynamical system (11), (12) we introduce four ratios of reaction rate parameters,

$$\vartheta_i = \frac{k_i^Q k_i^P}{d_i^Q d_i^P} \quad \text{and} \quad \phi_i = \frac{d_i^P}{k_i^P}, \quad i = 1, 2, \quad (13)$$

that simplify the expressions obtained from $\dot{q}_i = \dot{p}_i = 0$, $i = 1, 2$:

$$\bar{p}_i - \vartheta_i F_i(\bar{p}_j) = 0, \quad i = 1, 2, \quad j = 2, 1. \quad (14)$$

The binding functions are normalized, $0 \leq F_i \leq 1$, and hence the equilibrium concentrations of proteins are confined to values in the range $0 \leq \bar{p}_i \leq \vartheta_i$ with $i = 1, 2$. For mass action the binding functions are rational functions, $F_i(\bar{p}_j) =$

$N_i(\bar{p}_j)/D_i(\bar{p}_j)$ with N_i and D_i being two polynomials in \bar{p}_j , and then the two Eq. (14) can always be written as two coupled polynomials whose roots define the stationary points. Examples will be given in the forthcoming sections. The stationary values of the mRNA concentration are proportional to the stationary protein concentrations:

$$\bar{q}_i = \phi_i \bar{p}_i, \quad i = 1, 2. \quad (15)$$

Again we point at a difference in dimensions: $[\vartheta_i] = [m]$, whereas the ϕ_i 's are dimensionless. Stationary concentrations are completely defined by the two ratios of kinetic constants, ϑ_1 and ϑ_2 (and, of course, by the parameters in the functions F_1 and F_2).

Apart from an initial phase determined largely by the choice of the four initial values $q_i(0), p_i(0)$ ($i = 1, 2$), the projection of the trajectories $(q_1(t), q_2(t), p_1(t), p_2(t))$ onto the (q_1, q_2) subspace shows close similarity to that onto the (p_1, p_2) plane. For stability analysis it is sufficient therefore to consider the fixed points and their properties on either of the two subspaces. We choose the ‘protein’ subspace $\mathcal{P} = \{p_i; p_i \geq 0 \forall i = 1, 2\}$ since protein concentrations are calculated more directly. It is worth noticing that the positions of the stationary points, $\bar{P} = (\bar{p}_1, \bar{p}_2) \in \mathcal{P}$, depend only on ϑ_1 and ϑ_2 and not on all eight kinetic parameters. Substitution of $\bar{p}_2 = \vartheta_2 F_2(\bar{p}_1)$ yields the solution

$$\bar{p}_1 - \vartheta_1 F_1(\vartheta_2 F_2(\bar{p}_1)) = 0. \quad (16)$$

Eq. (16) leads to high-order polynomials for nonlinear binding functions which, nevertheless, are computed straightforwardly for general n for the simple binding functions (5). For activation–activation, activation–repression and repression–repression, we obtain

$$\bar{p}_1 \cdot \left(\bar{p}_1^{n-n} \vartheta_2^n - \bar{p}_1^{n-n-1} \vartheta_1 \vartheta_2^n + K_2 \cdot \sum_{k=0}^n \bar{p}_1^{n(n-k)} \binom{n}{k} K_1^k \right) = 0, \quad (17)$$

$$K_2 \cdot \left(\sum_{k=0}^n \bar{p}_1^{n(n-k)+1} \binom{n}{k} K_1^k \right) + (\bar{p}_1 - \vartheta_1) (\vartheta_2 K_1)^n = 0 \quad \text{and} \quad (18)$$

$$(\bar{p}_1 - \vartheta_1) K_2 \cdot \left(\sum_{k=0}^n \bar{p}_1^{n(n-k)} \binom{n}{k} K_1^k \right) + \bar{p}_1 \cdot (\vartheta_2 K_1)^n = 0, \quad (19)$$

respectively. The equilibrium concentration \bar{p}_2 is readily obtained from

$$\bar{p}_2 = \frac{\vartheta_2 \cdot \bar{p}_1^n}{K_1 + \bar{p}_1^n} \quad \text{for (17) and}$$

$$\bar{p}_2 = \frac{\vartheta_2 \cdot K_1}{K_1 + \bar{p}_1^n} \quad \text{for (18) and (19).}$$

It follows from Eq. (17) that the origin is always a fixed point for activation–activation systems, $\bar{P}_1 = (0, 0)$, corresponding to both genes silenced. The degree of the polynomials in \bar{p}_1 , $\pi_n = n^2 + 1$, increases with the square

of the Hill coefficient and thus already reaches 17 for $n = 4$. Nevertheless, we never obtained more than three or four real roots through numerical solution (for $n \leq 4$). Obviously, we have an even number of real roots for n odd (1 and 3) and an odd number of real roots for n even (2 and 4).

The high degree of the polynomials prohibits direct calculations based on Eqs. (17)–(19) but the expressions are suitable for computing, for example, the limits of the equilibrium concentrations for strong and weak binding, $\lim K_{1,2} \rightarrow 0$ and $\lim K_{1,2} \rightarrow \infty$, respectively. The results are shown in Table 1 and they correspond completely to the expectations. When the limits are taken for both constants simultaneously the limiting concentrations are independent of the Hill coefficient n —not unexpectedly since all functions $F_i(\bar{p}_j; K_j, n)$ approach either zero or one in these limits. Examples of individual dynamical systems will be discussed in Section 4 and therefore we mention only one general feature here: in the strong binding limit the combination activation–activation leads to two active genes or to silencing of both genes, whereas we have alternate activities—‘1’ active and ‘2’ silent or ‘1’ silent and ‘2’ active—in the repression–repression system. Weak binding, on the other hand, silences the genes in the **act–act** case and leads to full activities in **rep–rep** systems.

In the next Section 3.2 we shall again make use of Eqs. (17)–(19) and derive limits of functions for the strong binding case, which are applied to the analysis of the regulatory dynamics in parameter space.

3.2. Jacobian matrix

The dynamical properties of the ODEs (11), (12) are analyzed by means of the Jacobian matrix and its eigenvalues. For the combined vector of all variables, $\mathbf{x} = (x_1, \dots, x_4) = (q_1, q_2, p_1, p_2)$, the Jacobian matrix A has a useful block structure:

$$A = \left\{ a_{ij} = \frac{\partial \dot{x}_i}{\partial x_j} \right\} = \begin{pmatrix} Q_d & Q_k \\ P_k & P_d \end{pmatrix} = \begin{pmatrix} -d_1^Q & 0 & k_1^Q \frac{\partial F_1}{\partial p_1} & k_1^Q \frac{\partial F_1}{\partial p_2} \\ 0 & -d_2^Q & k_2^Q \frac{\partial F_2}{\partial p_1} & k_2^Q \frac{\partial F_2}{\partial p_2} \\ k_1^P & 0 & -d_1^P & 0 \\ 0 & k_2^P & 0 & -d_2^P \end{pmatrix}. \tag{20}$$

This block structure of matrix A largely facilitates the computation of the $2n$ eigenvalues (Marcus, 1987; Kovacs et al., 1999. Since the matrices Q_d and P_k commute, $Q_d P_k = P_k Q_d$, the relation

$$\begin{vmatrix} Q_d & Q_k \\ P_k & P_d \end{vmatrix} = |Q_d P_d - Q_k P_k|$$

holds. In certain cases, in particular for all forms of cyclic regulation of genes including cross-regulation of two genes, $\mathbf{G}_N \Rightarrow \mathbf{G}_1 \Rightarrow \mathbf{G}_2 \Rightarrow \dots \Rightarrow \mathbf{G}_N$ for arbitrary N (Schuster

Table 1 Protein concentrations in the strong and weak binding limits

System	Strong binding: $\lim K_j \rightarrow 0$			Weak binding: $\lim K_j \rightarrow \infty$		
	j	\bar{p}_1	\bar{p}_2	j	\bar{p}_1	\bar{p}_2
act–act ^a	1	0	0	1	0	0
		$\frac{\vartheta_1 \vartheta^n}{K_2 + \vartheta_2^n}$	ϑ_2			
	2	0	0	2	0	0
		ϑ_1	$\frac{\vartheta_2 \vartheta^n}{K_1 + \vartheta_1^n}$			
	1,2	0	0	1,2	0	0
		ϑ_1	ϑ_2			
act–rep	1	0	0	1	$\frac{\vartheta_1 \vartheta_2^n}{K_2 + \vartheta_2^n}$	ϑ_2
	2	ϑ_1	$\frac{K_1}{K_1 + \vartheta_1^n}$	2	0	ϑ_2
	1,2	0	0	1,2	0	ϑ_2
rep–rep	1	ϑ_1	0	1	$\frac{K_2}{K_2 + \vartheta_2^n}$	ϑ_2
	2	0	ϑ_2	2	ϑ_1	$\frac{K_1}{K_1 + \vartheta_1^n}$
	1,2	ϑ_1	0	1,2	ϑ_1	ϑ_2
		0	0			
		0	ϑ_2			

The limits were calculated from Eqs. (17)–(19) by taking the limits $\lim K_1 \rightarrow 0$ and/or $\lim K_2 \rightarrow 0$ or $\lim K_1 \rightarrow \infty$ and/or $\lim K_2 \rightarrow \infty$, respectively.

^aThe solution ($\bar{p}_1 = 0, \bar{p}_2 = 0$) is a double root in the strong binding limit.

et al., 2006), the secular equation, $|A - \varepsilon E| = 0$ (where E is unit matrix), is of the form⁵

$$(\varepsilon + d_1^Q)(\varepsilon + d_2^Q)(\varepsilon + d_1^P)(\varepsilon + d_2^P) + D = 0 \quad \text{with}$$

$$D = k_1^Q k_2^Q k_1^P k_2^P \begin{vmatrix} 0 & \frac{\partial F_1}{\partial p_2} \\ \frac{\partial F_2}{\partial p_1} & 0 \end{vmatrix} = -k_1^Q k_2^Q k_1^P k_2^P \frac{\partial F_1}{\partial p_2} \cdot \frac{\partial F_2}{\partial p_1}. \quad (21)$$

Since D determines the eigenvalues of the Jacobian A we call it the *regulatory determinant* of the dynamical system: knowledge of D is sufficient to analyze the stability of fixed points and to calculate the parameter values at bifurcation points.

At $D = 0$ the eigenvalues of the Jacobian are the set of all four negative degradation rate constants, $-d_i^Q$ and $-d_i^P$ ($i = 1, 2$), ordered by value: $\varepsilon_1 = -\min\{d_1^Q, d_2^Q, d_1^P, d_2^P\}$ is the largest and $\varepsilon_4 = -\max\{d_1^Q, d_2^Q, d_1^P, d_2^P\}$ is the smallest eigenvalue of A . In the non-degenerate case, i.e. when all degradation rate parameters are different, the eigenvalues correspond to four points on the negative (reciprocal time) axis represented by the ordinate axis in Fig. 2. For a fixed point $\bar{P} \in \mathcal{P}$ with $D = 0$ this implies asymptotic stability. Non-generic cases with double or multiple real roots at $D = 0$ imply also asymptotic stability; only the analytical continuation then yields one or more complex conjugate pairs of eigenvalues with negative real parts.

Fig. 2 shows a plot of the individual eigenvalues as functions of D . All curves together form a quartic equation rotated by $\pi/2$, and the shape of the fourth-order polynomial determines the bifurcation pattern. At increasing negative values $D < 0$, i.e. in the negative D direction in Fig. 2, the two eigenvalues ε_2 and ε_3 approach each other and, at some point, $D = D_1$ this pair of real eigenvalues merges and becomes a complex conjugate pair of eigenvalues. The largest and the smallest eigenvalue, ε_1 and ε_4 , remain single-valued. Because of the shape of a quartic equation, the largest eigenvalue ε_1 increases and the lowest eigenvalue ε_4 decreases in the negative D direction. The condition $\varepsilon_1 = 0$ occurs at the position $D = \bar{D}_{\text{oneD}}$, which is defined by

$$\bar{D}_{\text{oneD}} = -d_1^Q \cdot d_2^Q \cdot d_1^P \cdot d_2^P. \quad (22)$$

Here, the fixed point $\bar{P}(\bar{p}_1(D), \bar{p}_2(D))$ changes stability and becomes unstable for $D < \bar{D}_{\text{oneD}}$. Since only one eigenvalue is involved, the corresponding bifurcation is one-dimensional, for example, a transcritical, a saddle-node or a pitchfork bifurcation (For examples see Section 4). From

⁵Generalization to N genes is straightforward: we have $2N$ variables and $2N$ factors rather than four, and the function D depends on N protein concentrations.

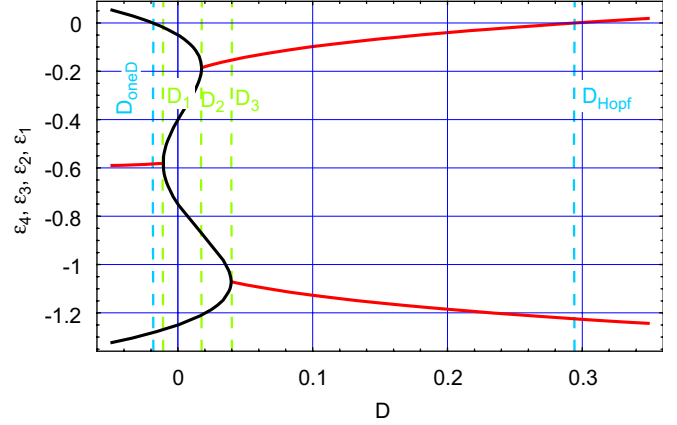


Fig. 2. Eigenvalues of the Jacobian matrix (20). The four eigenvalues of a two-gene system, $\varepsilon_1, \varepsilon_2, \varepsilon_3$ and ε_4 , are plotted as functions of D around the point $D = 0$ as reference. The dimension of the ordinate axis is reciprocal time, $[t^{-1}]$. At $D = 0$ and different values of d_1^Q, d_2^Q, d_1^P and d_2^P we observe four negative real eigenvalues of the Jacobian, which are turning into complex conjugate pairs at the values $D = D_1, D = D_2$ and $D = D_3$. At D_{oneD} and at D_{Hopf} the fixed point changes stability. The one dimensional bifurcation lies at negative values of D since $D_{\text{oneD}} < 0$, whereas $D_{\text{Hopf}} > 0$, and thus the Hopf bifurcation appears always at positive D values. Color code: Real eigenvalues are drawn in black and the real parts of complex conjugate pairs of eigenvalues are shown as red lines.

Eq. (22) follows the condition for the stability of fixed points with negative D :

$$\bar{P} \text{ with } D(\bar{p}_1, \bar{p}_2) < 0 \text{ is stable iff } \vartheta_1 \cdot \vartheta_2 \cdot \frac{\partial F_1}{\partial p_2} \cdot \frac{\partial F_2}{\partial p_1} < 1. \quad (23)$$

The stability of fixed points \bar{P} with negative values of D , like their positions (\bar{p}_1, \bar{p}_2) , is determined by the two parameter combinations ϑ_1, ϑ_2 , and the derivatives of the binding functions F_1 and F_2 . For $D < \bar{D}_{\text{oneD}}$ the fixed point is unstable, and the largest eigenvalue ε_1 is real and positive.

In the direction of positive values, $D > 0$, the eigenvalues approach each other in pairs: $(\varepsilon_1, \varepsilon_2)$ and $(\varepsilon_3, \varepsilon_4)$. If the two eigenvalues in such a pair become equal at some value $D > 0$, at the values D_2 and D_3 in Fig. 2, the two negative real eigenvalues merge and give birth to a complex conjugate pair with negative real part. The real parts of the two complex conjugate pairs behave like the upper part of a quadratic equation rotated by $\pi/2$ and hence the real part of the pair formed by the two larger eigenvalues, $\lambda_1 = \Re(\varepsilon_1, \varepsilon_2)$, increases with increasing D . As indicated in Fig. 2 it may cross zero at some point $D = \bar{D}_{\text{Hopf}}$. There the fixed point loses stability through a Hopf bifurcation. The value of D can be computed (see the Appendix) and one obtains

$$\bar{D}_{\text{Hopf}} = \frac{(d_1^Q + d_2^Q)(d_1^Q + d_1^P)(d_1^Q + d_2^P)(d_2^Q + d_1^P)(d_2^Q + d_2^P)(d_1^P + d_2^P)}{(d_1^Q + d_2^Q + d_1^P + d_2^P)^2}. \quad (24)$$

If $0 \leq D < \bar{D}_{\text{Hopf}}$ is fulfilled for some fixed point $\bar{P} \in \mathcal{P}$ with positive D , the fixed point is stable:

$$\bar{P} \text{ with } D(\bar{p}_1, \bar{p}_2) > 0 \text{ is stable iff } -\frac{k_1^Q \cdot k_2^Q \cdot k_1^P \cdot k_2^P}{\bar{D}_{\text{Hopf}}} \frac{\partial F_1}{\partial p_2} \cdot \frac{\partial F_2}{\partial p_1} < 1. \quad (25)$$

\bar{P} is unstable for $D > \bar{D}_{\text{Hopf}}$, and at $D = \bar{D}_{\text{Hopf}}$ we expect a marginally stable point with concentric orbits in a (small) neighborhood of \bar{P} . In summary, all fixed points $\bar{P} \in \mathcal{P}$ are asymptotically stable in the range $\bar{D}_{\text{oneD}} < D < \bar{D}_{\text{Hopf}}$ (see the Appendix), all four eigenvalues are real between $D_1 < D < D_2$.

Eq. (21) can be solved easily if all degradation rate parameters are equal, $d_1^Q = d_n^Q = d_1^P = d_2^P = d$:

$$(\varepsilon + d)^4 + D = 0 \implies \varepsilon_i = -d + \sqrt[4]{-D}, \quad i = 1, \dots, 4.$$

Similarly, the eigenvalues are readily calculated if all RNA and all protein degradation rates are the same: $d_1^Q = d_2^Q = d^Q$ and $d_1^P = d_2^P = d^P$ yields

$$(\varepsilon + d^Q)(\varepsilon + d^P) = \pm \sqrt{-D},$$

where the computation boils down to solving two quadratic equations.

For a given fixed point the function $D(\bar{p}_1, \bar{p}_2)$ determines the bifurcation behavior of the system. In all examples with simple binding functions of type (5), the derivatives $\partial F_1 / \partial p_2$ and $\partial F_2 / \partial p_1$ are either positive or negative for all (non-negative) values of the concentrations p_1 and p_2 . Indeed we find $D(\bar{p}_1, \bar{p}_2) \leq 0$ for activation of both genes (**act-act**) and repression of both genes (**rep-rep**), whereas combinations of activation and repression, (**act-rep**) and (**rep-act**), yield always non-negative values, $D(\bar{p}_1, \bar{p}_2) \geq 0$. Calculation of the regulatory determinant for arbitrary n is straightforward and yields

$$D = \mp k_1^Q k_2^Q k_1^P k_2^P \frac{n^2 K_1 K_2 \bar{p}_1^{n-1} \bar{p}_2^{n-1}}{(K_1 + \bar{p}_1^n)(K_2 + \bar{p}_2^n)}. \quad (26)$$

Here, the minus sign holds for **act-act** and **rep-rep** whereas the plus sign is true for **act-rep** and **rep-act**. In the **act-act** case, insertion of the coordinates of the fixed point at the origin, $\bar{P}_1 = (0, 0)$, yields the very general result that \bar{P}_1 is always stable for $n \geq 2$ because we obtain $D = 0$ in this case.

Eqs. (17)–(19) are useful in searching parameter space for bifurcations. Auxiliary variables can be used to define manifolds on which the search is carried out. As an illustrative example we consider the search for a Hopf bifurcation along the one-dimensional manifold defined by $(k_1^Q = \chi_1 \cdot s, k_2^Q = \chi_2 \cdot s, K_1 = \lambda_1/s, K_2 = \lambda_2/s)$ in the **act-rep** system (18). From these relations follows $\vartheta_i = \delta_i s$ with $\delta_1 = (k_1^P / (d_1^Q d_1^P)) \chi_1$ and $\delta_2 = (k_2^P / (d_2^Q d_2^P)) \chi_2$, respectively. The computation of the equilibrium concentrations for large s is straightforward and yields for $n > 1$ (an

example for $n = 1$ is presented in Section 4.2)

$$\bar{p}_1 = \alpha_1 \cdot s^{2/(n^2+1)} \quad \text{with } \alpha_1 = \left(\frac{\delta_1 (\delta_2 \lambda_1)^n}{\lambda_2} \right)^{1/(n^2+1)} \quad \text{and}$$

$$\bar{p}_2 = \alpha_2 \cdot s^{-2n/(n^2+1)} \quad \text{with } \alpha_2 = \left(\frac{\lambda_1}{(\delta_1 (\delta_2 \lambda_1)^{n^3/(n^2+1)})} \right)^{n/(n^2+1)}.$$

Insertion into the expression for the regulatory determinant leads to exact cancellation of the powers of s and we find in the

$$\text{limit of large } s: D_{\text{lim}} \approx k_1^Q k_2^Q k_1^P k_2^P \frac{n^2}{\vartheta_1 \vartheta_2} = d_1^Q d_2^Q d_1^P d_2^P n^2. \quad (27)$$

This value has to be compared with the condition for the occurrence of a Hopf bifurcation (24). As an example of an application we analyze the function

$$H(d_1^Q, d_2^Q, d_1^P, d_2^P, n) = D_{\text{lim}} / \bar{D}_{\text{Hopf}}$$

$$= n^2 \frac{d_1^Q d_2^Q d_1^P d_2^P (d_1^Q + d_2^Q + d_1^P + d_2^P)^2}{(d_1^Q + d_2^Q)(d_1^Q + d_1^P)(d_1^Q + d_2^P)(d_2^Q + d_1^P)(d_2^Q + d_2^P)(d_1^P + d_2^P)} \quad (28)$$

to show whether or not **act-rep** systems with Hill coefficient $n > 1$ can undergo a Hopf bifurcation at certain parameter values and sustain undamped oscillations. A value $H > 1$ indicates that a limit cycle exists for sufficiently large values of s . The maximum of H is computed by partial differentiation with respect to the degradation rate constants⁶

$$\left(\frac{\partial H}{\partial d_1^Q} \right) = 0 \implies (d_1^Q)^3 (d_2^Q + d_1^P + d_2^P) + (d_1^Q)^2 ((d_2^Q)^2 + (d_1^P)^2 + (d_2^P)^2) - 3d_1^Q (d_2^Q d_1^P d_2^P) - d_2^Q d_1^P d_2^P (d_2^Q + d_1^P + d_2^P) = 0.$$

This cubic equation is hard to analyze but the question raised here can be answered without explicit solution. We assume $d_2^Q = d_1^P = d_2^P = d$ and obtain

$$(d_1^Q - d)(d_1^Q + d)^2 = 0 \implies d_1^Q = d \quad \text{and}$$

$$H(d, d, d, d, n) = \frac{n^2}{4}.$$

By numerical inspection we showed that any deviation from uniform degradation rate parameters leads to a smaller value for the maximum of H . In the strong binding limit the **act-rep** system with $n = 2$ is confined to values $H \leq 1$ and indeed no limit cycle has been observed. Systems with $n \geq 3$, however, show values of $H_{\text{max}} = n^2/4 > 1$ in certain regions of parameter space, and they do indeed sustain undamped oscillations. For the fixed point in the positive quadrant the D value increases from weak to

⁶Since function (28) is symmetric with respect to all four rate parameters all four partial derivatives have identical analytical expressions.

strong binding and this completes the arguments for the non-existence of undamped oscillation for $n = 2$.

3.3. Basal transcription

The basal state shown in Fig. 1 is often characterized as ‘leaky transcription’ since it leads to low levels of mRNA. In order to take basal activity formally into account we add (small) constant terms, γ_1 and γ_2 , to the binding functions (5) and find for activation and repression

$$\begin{aligned} F_1^{(\text{act})}(p_2) &= \gamma_1 + \frac{p_2^n}{K_2 + p_2^n} = \frac{\gamma_1 K_2 + (1 + \gamma_1)p_2^n}{K_2 + p_2^n}, \\ F_1^{(\text{rep})}(p_2) &= \gamma_1 + \frac{K_2}{K_2 + p_2^n} = \frac{(1 + \gamma_1)K_2 + \gamma_1 p_2^n}{K_2 + p_2^n}, \\ F_2^{(\text{act})}(p_1) &= \gamma_2 + \frac{p_1^n}{K_1 + p_1^n} = \frac{\gamma_2 K_1 + (1 + \gamma_2)p_1^n}{K_1 + p_1^n}, \\ F_2^{(\text{rep})}(p_1) &= \gamma_2 + \frac{K_1}{K_1 + p_1^n} = \frac{(1 + \gamma_2)K_1 + \gamma_2 p_1^n}{K_1 + p_1^n}. \end{aligned} \quad (29)$$

Basal transcription activity is readily incorporated into the analytic procedure described here. The computation of fixed points is straightforward although it involves more terms. Since the constant terms vanish through differentiation, the regulatory determinant and the whole Jacobian matrix depend on basal transition only via the changes in the positions of the fixed points, $\bar{P}_k = (\bar{p}_1^{(k)}, \bar{p}_2^{(k)})$. The rate coefficients γ_i measure basal transcription activity relative to the fully developed regulated activity, $F_i(p_j) = 1$. It is worth noticing that the rate coefficients γ_i are dimensionless—as the binding functions $F_i(p_j)$ are—and, therefore, the full rate parameters for leaky transcription are obtained by multiplication: $k_i^Q \gamma_i$.

For gene regulation leaky transcription is most important in cases where both genes are activated. Activation without basal transcription allows for irreversible silencing of both genes since they can be turned off completely and after degradation of the activator proteins the system cannot recover its activity. In mathematical terms the origin, $\bar{P}(0, 0)$, is an asymptotically stable fixed point. Basal transcription changes this situation because some low-level protein synthesis is always going on and the origin is a fixed point no longer. In the forthcoming Section 4 we shall consider several examples where leaky transcription has been included.

4. Selected examples

Examples for activation and repression were considered for non-cooperative binding ($n = 1$) as well as for cooperative binding ($n \geq 2$) up to $n = 4$. In addition, examples were included where intermediate complexes are active in transcription. In agreement with the limits of stationary protein concentrations (Table 1) the calculations reported in this section show that at low ratios of ϑ/K all systems sustain asymptotically stable stationary states in the positive quadrant including the origin, all except very few (see Table 4) undergo a bifurcation at some larger value of ϑ/K and reach,

thereafter, the biologically relevant or *regulated* state. The changes in the dynamical patterns in parameter space are investigated by means of an auxiliary variable s that defines a path in parameter space (see Section 3.2). The range in parameter space with low values of ϑ/K is characterized by low ratios of reaction rate parameters and/or high dissociation parameters of the regulatory complexes, which is tantamount to low binding constants or low affinities. It will be denoted here as the *unregulated regime*, because the dynamics in this range is not suitable for regulatory functions. In contrast, the parameter range with high ratios of ϑ/K above the bifurcation value will be called the *regulated regime* since bistability or oscillations (or sometimes both) occur in this region. In the cases discussed here we shall investigate paths through parameter space that lead from the unregulated to the regulated regime which can be achieved, for example, by assuming $\vartheta \propto s$ and $K \propto s^{-1}$.⁷ For all pure activation–activation and repression–repression systems the function D is non-positive and hence Hopf bifurcations, and limit cycles derived from them, can be excluded. Instead one-dimensional bifurcations, transcritical, saddle-node and pitchfork bifurcations, are observed, the latter two resulting in bistability of the system. Activation–repression yields non-negative values of D and hence the systems may reach oscillatory states via the Hopf bifurcation mechanism. Cases in which intermediate complexes are active in transcription were included as examples of regulatory determinants D that can adopt positive as well as negative values and therefore may sustain oscillations and bistability at different parameter values.

For integer Hill coefficients $n \geq 2$ the binding curves have sigmoidal shape and multiple steady states or oscillatory behavior emerges. As mentioned in Section 3.1 the polynomials for the computation of the positions of fixed points have an odd or even number of real solutions for even or odd Hill coefficients n (two or four solutions for n odd and one or three solutions for n even). Despite the high degrees of the polynomials in \bar{p}_1 or \bar{p}_2 ($n^2 + 1$) we did not detect more stationary states up to $n = 4$. Although our searches of the high-dimensional parameter spaces were not exhaustive, it is unlikely that fixed points remained unnoticed. The small number of distinct states causes the dynamic patterns of the cooperative systems with different $n \geq 2$ to be qualitatively similar, with an exception being activation–repression where the characteristic nonlinear behavior, oscillations, is observed only for $n \geq 3$.

4.1. Activation–activation cases

The binding functions for these cases are

$$F_1(p_2) = \gamma_1 + \frac{p_2^n}{K_2 + p_2^n} \quad \text{and} \quad F_2(p_1) = \gamma_2 + \frac{p_1^n}{K_1 + p_1^n}. \quad (30)$$

⁷Considering the limits, $\lim_{s \rightarrow 0} \bar{P}_k(s)$ and $\lim_{s \rightarrow \infty} \bar{P}_k(s)$ with $k = 1, 2, \dots$, is important for all fixed points, for example, in order to recognize equivalent and non-equivalent paths through parameter space.

The discussion of activation–activation cases is organized in three subsections: (i) non-cooperative binding ($\gamma_1 = \gamma_2 = 0, n = 1$), (ii) cooperative binding ($\gamma_1 = \gamma_2 = 0, n \geq 2$) and (iii) leaky transcription ($\gamma_1 \neq 0, \gamma_2 \neq 0$).

Non-cooperative binding: The search for stationary points leads to two solutions:

$$\bar{P}_1 = (0, 0) \quad \text{and} \quad \bar{P}_2 = \left(\frac{\vartheta_1 \vartheta_2 - K_1 K_2}{\vartheta_2 + K_2}, \frac{\vartheta_1 \vartheta_2 - K_1 K_2}{\vartheta_1 + K_1} \right). \quad (31)$$

For $\vartheta_1 \vartheta_2 > K_1 K_2$ the fixed point \bar{P}_2 is inside the positive quadrant of protein space and it is stable as can be readily verified by means of Eq. (23). At the critical value $\vartheta_1 \vartheta_2 = K_1 K_2$ the two fixed points exchange stability as required for a transcritical bifurcation. Although the state at negative concentrations is irrelevant for gene regulation, its existence explains the instantaneous onset of gene transcription at the bifurcation point, above which ($s > s_{\text{oneD}}$) the origin becomes unstable. A special example is shown in Fig. 3: the path through parameter space is defined by $K_1 = 0.5/s$ and $K_2 = 2.5/s$ (the other parameters are summarized in the caption of Fig. 3). The limits for the position of the two fixed points are: (i) \bar{P}_1 stays at the origin for all s and (ii) for \bar{P}_2 we compute $\lim_{s \rightarrow 0} \bar{P}_2 = (-\infty, -\infty)$ and $\lim_{s \rightarrow \infty} \bar{P}_2 = (2, 2)$.

It is worth considering the physical meaning of the stability condition for \bar{P}_2 . The parameters ϑ are the squares of the geometric means of the formation rate constants divided by the degradation rate constants, the K 's are the reciprocal binding constants and, hence, both genes are active for sufficiently large formation rate parameters and high binding affinities. The combination activation–activation with non-cooperative binding shows modest regulatory properties. It sustains two states: (i) a regulated state where both genes are transcribed and (ii) a state of ‘extinction’ with both genes silenced.

Cooperative binding: For the simplest example, $n = 2$, the expansion of Eq. (16) yields a polynomial of degree five. Numerical solution leads to one or three solutions in the positive quadrant including the origin, which correspond to one or three steady states. The origin represents one fixed point, $\bar{P}_1 = (0, 0)$, that in contrast to the non-cooperative system is always stable.⁸ Searching parameter space in the direction of increasing transcription rate parameters, ($k_1^Q = \chi_1 \cdot s, k_2^Q = \chi_2 \cdot s$), and/or decreasing dissociation constants of regulatory complexes, ($K_1 = \lambda_1/s, K_2 = \lambda_2/s$), yields a saddle-node bifurcation when the condition $D = \bar{D}_{\text{oneD}}$ of Eq. (22) is fulfilled (Fig. 4). At this bifurcation point, which separates the unregulated regime (with the origin being the only stable state) from the regulated regime, two new fixed points \bar{P}_2 and \bar{P}_3 appear and branch off, thereby fulfilling the conditions $D < \bar{D}_{\text{oneD}}$ and $D > \bar{D}_{\text{oneD}}$, respectively. The fixed point \bar{P}_2 is

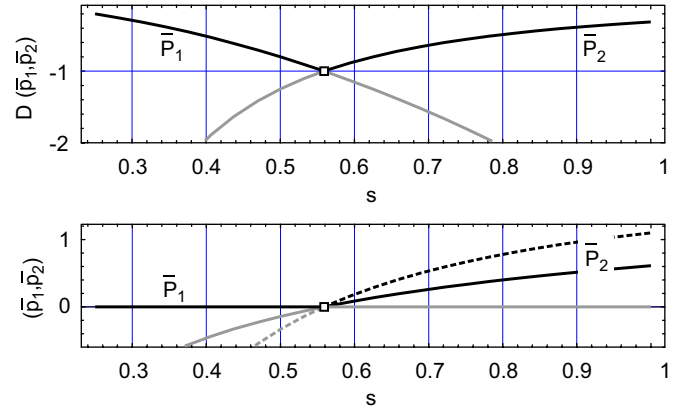


Fig. 3. Position and stability of the two fixed points in the two-gene non-cooperative activation–activation system according to Eq. (31). The upper part of the figure shows the regulatory determinant D as a function of the auxiliary variable s for both fixed points \bar{P}_1 and \bar{P}_2 (stable fixed points: black line; unstable fixed points: gray line). According to Eq. (22) we observe a transcritical bifurcation at the value $s = s_{\text{oneD}} = \frac{\sqrt{5}}{4} = 0.559$, which is indicated by \square . Both D functions adopt the value $\bar{D}_{\text{oneD}} = -1$ and exchange stability at this point. The fixed point at the origin, \bar{P}_1 , is asymptotically stable for $s < s_{\text{oneD}}$ whereas \bar{P}_2 shows stability above this value. The lower plot presents the position of the two fixed points as a function of s (coordinates: \bar{p}_1 full line, \bar{p}_2 broken line if different from \bar{p}_1 ; stability of the fixed point is indicated by black curves, instability by gray curves). The fixed point \bar{P}_2 becomes stable when it enters the positive orthant. Parameter values: $k_1^Q = k_2^Q = 1, K_1 = 0.5/s, K_2 = 2.5/s, k_1^P = k_2^P = 2$ and $d_1^Q = d_2^Q = d_1^P = d_2^P = 1$.

unstable—at least for some range in parameter space—whereas the fixed point \bar{P}_3 is asymptotically stable since D can only adopt negative signs (examples with no sign restriction on D are discussed in Section 4.5 dealing with cases intermediate between activation and repression). Raising the Hill coefficient from $n = 2$ to 3 and to 4 has little effect on the position of the bifurcation point. As shown in Table 2 we find somewhat smaller values of s at the bifurcation point for the higher Hill coefficients, but the changes are much smaller than for either the activation–repression or the repression–repression system. In addition this weak dependence may be replaced by even weaker or no dependence on n when the implementation of the auxiliary variable s is changed.

Leaky transcription: The effect of leaky transcription is illustrated in Figs. 5 and 6. Leaky transcription commonly occurs at very low levels and accordingly we choose γ to lie in the range $1 \times 10^{-3} < \gamma < 0.1$.⁹ For $\gamma_i > 0$ ($i = 1, 2$) the fixed point at the origin is shifted either into the negative or into the positive quadrant such that exactly one fixed point is in each quadrant. The fixed point in physical protein space is always asymptotically stable, the one outside physical space is unstable. The scenario shown in Fig. 5

⁸This result follows straightforwardly from a computation of the derivatives in the Jacobian, which yields $D = 0$ at the origin for all Hill coefficients $n > 1$.

⁹The rate coefficient γ is dimensionless and expresses leaky transcription relative to controlled transcription at its highest level, $F_i(p_j) = 1$ (see Section 3.3).

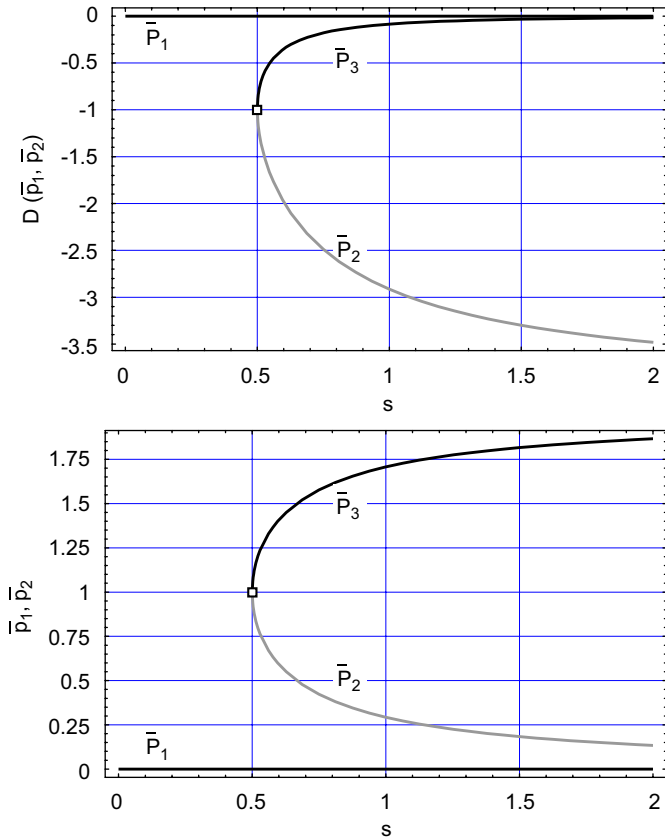


Fig. 4. Position and stability of the fixed points in the two-gene cooperative activation–activation system with Hill coefficient $n = 2$. Positions and stabilities of fixed points are plotted as functions of the auxiliary variable s , which determines the binding constants: $K_1 = K_2 = 0.5/s$. The upper part of the figure shows the regulatory determinant as a function of the auxiliary variable s (stable fixed points: black line; unstable fixed points: gray line). One fixed point situated at the origin, $\bar{P}_1 = (0, 0)$, is stable for all parameter values. The systems shows a saddle-node bifurcation at $s = 0.5$ through which the two fixed points, \bar{P}_2 and \bar{P}_3 , are created (\square). The lower part presents the positions of the fixed points as functions of s (coordinates: $\bar{p}_1 = \bar{p}_2$; stability of the fixed point is indicated by black curves, instability by gray curves). Choice of the other parameters: $k_1^Q = k_2^Q = 2$, $k_1^P = k_2^P = d_1^Q = d_2^Q = d_1^P = d_2^P = 1$.

starts out from the position of the transcritical bifurcation in the limit $\gamma \rightarrow 0$. Accordingly, two states fulfilling the criteria mentioned above emerge at $\gamma > 0$, the unstable state appears in the negative quadrant, $\bar{P}_1 = (\bar{p}_1^{(1)} < 0, \bar{p}_2^{(1)} < 0)$, and the stable fixed point is always inside the positive quadrant, $\bar{P}_2 = (\bar{p}_1^{(2)} > 0, \bar{p}_2^{(2)} > 0)$.

The plots in Fig. 6 illustrate the influence of weak basal transcription on the activation–activation regulatory system around the transcritical bifurcation point of the unperturbed system. An auxiliary variable is defined by $K_1 = 0.5/s$ and $K_2 = 2.5/s$ (the other parameter values are given in the caption of Fig. 6). For $\gamma_1 = \gamma_2 = 0$ a transcritical bifurcation is observed at $s = 0.56$. Small gamma values give rise to *avoided crossing*: at some distance from the virtual crossing point the two states are very close to those of the pure activation system and the

continuation of these states at the other side of the virtual bifurcation point is readily recognized. The splitting for increasing $\gamma \geq 0$ at exactly this point was shown in the previous Fig. 5.

The cooperative case of activation ($n = 2$) with leaky transcription provides an illustrative example of a system with two saddle-node bifurcations, $(s_{\text{oneD}})_1$ and $(s_{\text{oneD}})_2$, which gives rise to hysteresis. Fig. 7 presents the fixed points as functions of spontaneous transcription rate parameter γ . In this figure the parameters were chosen such that the system has only one fixed point at $\lim \gamma \rightarrow 0$, the stable origin. With increasing values of γ the system undergoes a saddle-node bifurcation that leads to the regulated regime with two asymptotically stable fixed points, one at high and one at low stationary protein concentrations, separated by a saddle. Further increase in γ , however, leads to a second saddle-node bifurcation that annihilates the stable state originating from the origin together with the unstable saddle. The state that eventually remains is the high-activity state (both genes active) which originates in the first saddle-node bifurcation.

As shown in Fig. 7 the sequence of bifurcations gives rise to hysteresis in the range between the two bifurcation points, $(s_{\text{oneD}})_1 < s < (s_{\text{oneD}})_2$. Coming from high values of γ the system stays in the high-protein-concentration branch (as long as it is not shifted to the low-concentration state by fluctuations). The low-protein-concentration branch, on the other hand, is reached from s values below $(s_{\text{oneD}})_1$.

The existence of a single stable state at high values of s and with high protein concentrations is easy to interpret in the light of reaction kinetics: with increasing γ values spontaneous transcription will, at some point, dominate and then only the non-regulated stationary state exists. This situation, however, is unlikely to occur in realistic biological systems, because unregulated transcription is common at very low levels only. The second saddle-node bifurcation—although not natural—could well be of interest for the design of artificial regulatory systems since it allows for up and down regulation of gene activity in an intermediate range.

4.2. Activation–repression cases

The binding functions for these case are

$$F_1(p_2) = \gamma_1 + \frac{p_2^n}{K_2 + p_2^n} \quad \text{and} \quad F_2(p_1) = \gamma_2 + \frac{K_1}{K_1 + p_1^n}. \quad (32)$$

The discussion of activation–repression cases is organized in two subsections: (i) non-cooperative binding ($\gamma_1 = \gamma_2 = 0$, $n = 1$) and (ii) cooperative binding ($\gamma_1 = \gamma_2 = 0$, $n \geq 2$). Leaky transcription ($\gamma_1 \neq 0, \gamma_2 \neq 0$) will be mentioned later in a comparison of all different regulation scenarios.

Non-cooperative binding: The conditions of stationary concentrations lead to a quadratic equation with two

Table 2
Dependence of the bifurcation point on the Hill coefficient n

System	Bifurcation type	Parameter variation	Variable s at bifurcation		
			$n = 2$	$n = 3$	$n = 4$
act-act^a	Saddle-node	$K_1 = K_2 = 0.5/s^b$	0.5	0.422	0.296
act-rep	Hopf	$K_1 = K_2 = 0.5/s^b$	–	2.772	0.5
rep-rep	Pitchfork ^c	$K_1 = K_2 = 0.5/s^b$	0.5	0.106	0.033

The value of the auxiliary variable s at the bifurcation point that separates the unregulated regime and the regulated regime is compared for different cooperative regulation modes and Hill coefficients $n = 2, 3, 4$. In order to allow for comparison equivalent paths through parameter space were chosen for all three classes of systems.

^aIn case of **act-act** other paths through parameter space lead to small or almost vanishing dependencies of the bifurcation value of s on the Hill coefficient n , for example, we found $s = 0.79, 0.81, 0.78$ for $n = 2, 3, 4$, $k_1^Q = k_2^Q = 2 \cdot s$, $K_1 = K_2 = 0.5/s$ and $s = 1, 0.96, 0.90$ for $k_1^Q = k_2^Q = 2 \cdot s$, $K_1 = K_2 = 1/s$, respectively (all other parameters being one).

^bThe other parameter values were: $k_1^Q = k_2^Q = 2$ and $k_1^P = k_2^P = d_1^Q = d_2^Q = d_1^P = d_2^P = 1$.

^cThe pitchfork bifurcation becomes a saddle-node bifurcation, when the symmetry consisting of identical parameters for genes 1 and 2 is broken (see Figs. 12 and 13).

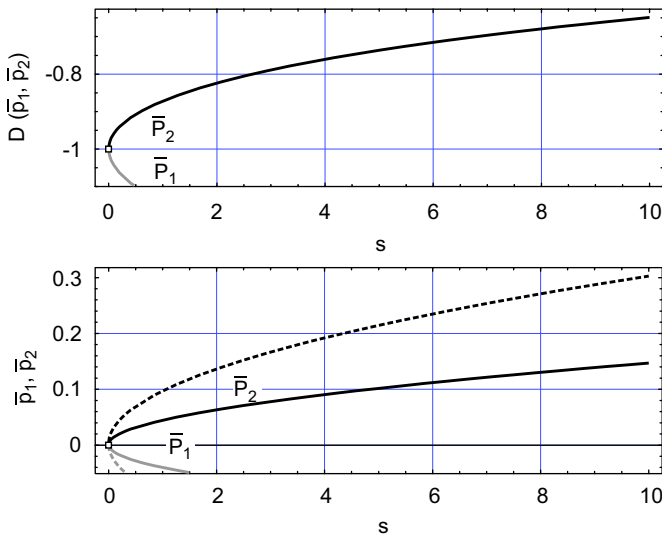


Fig. 5. Position and stability of the two fixed points in the two-gene non-cooperative activation-activation system with leaky transcription: γ -dependence. Leaky transcription is introduced into the system exactly at the transcritical bifurcation point (\square). The upper plot shows $D(\bar{p}_1, \bar{p}_2)$ for both fixed points as a function of an auxiliary variable s , which measures the extent of basal transcription, $\gamma_1 = \gamma_2 = 0.001 \cdot s$ (stable fixed point: black line; unstable fixed point: gray line). The lower plot presents the positions of the two fixed points (coordinates: \bar{p}_1 full line, \bar{p}_2 broken line if different from \bar{p}_1 ; stability of the fixed point is indicated by black curves, instability by gray curves). For $s > 0$ the fixed point \bar{p}_1 lies in the negative quadrant and is unstable, $D < -1$. The fixed point \bar{P}_2 is always situated in the physical protein space, the positive quadrant, and it is asymptotically stable since $0 \geq D \geq -1$ is fulfilled. Choice of parameters: $k_1^Q = k_2^Q = 1$, $K_1 = 0.892857$, $K_2 = 4.464286$, $k_1^P = k_2^P = 1$, $d_1^Q = d_2^Q = 2$ and $d_1^P = d_2^P = 1$.

solutions:

$$\bar{p}_1 = -\frac{1}{K_2} (K_1(\vartheta_2 + K_2) \pm \sqrt{K_1^2(\vartheta_2 + K_2)^2 + 4\vartheta_1 K_1 \vartheta_2 K_2}). \quad (33)$$

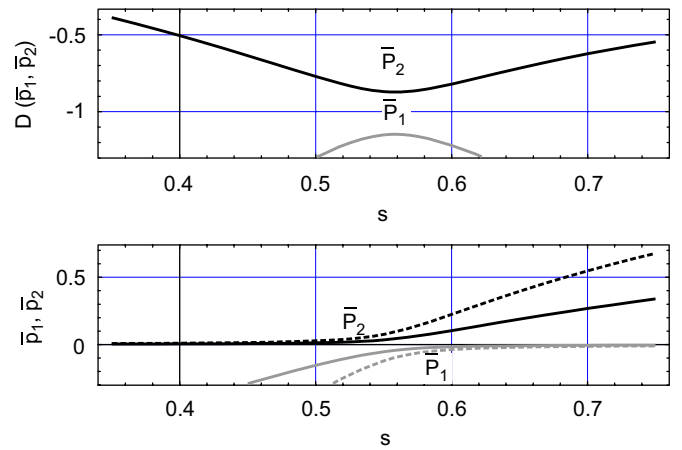


Fig. 6. Position and stability of the two fixed points in the two-gene non-cooperative activation-activation system with leaky transcription: K -dependence. In contrast to Fig. 5 basal transcription occurs at a constant rate $\gamma_1 = \gamma_2 = 0.001$ as a function of the equilibrium parameters, $K_1 = 0.5/s$ and $K_2 = 2.5/s$. The upper plot shows $D(\bar{p}_1, \bar{p}_2)$ for both fixed points as a function of an auxiliary variable s in the neighborhood of the transcritical bifurcation at $s = 0.56$ for $\gamma_1 = \gamma_2 = 0$ (stable fixed point: black line; unstable fixed point: gray line). The lower plot presents the positions of both points in the same range of s (coordinates: \bar{p}_1 full line, \bar{p}_2 broken line if different from \bar{p}_1 ; stability of the fixed point is indicated by black curves, instability by gray curves). For $s > 0$ the fixed point \bar{P}_1 lies in the negative quadrant and is unstable, $D < -1$. The fixed point \bar{P}_2 is always situated in the physical protein space, the positive quadrant, and it is asymptotically stable since $0 \geq D \geq -1$ is fulfilled. Choice of other parameters: $k_1^Q = k_2^Q = 1$, $k_1^P = k_2^P = 1$, $d_1^Q = d_2^Q = 2$ and $d_1^P = d_2^P = 1$.

This equation has one positive and one negative solution for \bar{p}_1 . For known \bar{p}_1 the second protein concentration is calculated from

$$\bar{p}_2 = \frac{\vartheta_2 K_1}{K_1 + \bar{p}_1}.$$

Combining this equation with $\bar{p}_1 = \vartheta_1 \bar{p}_2 / (K_2 + \bar{p}_2)$ allows us to prove that both variables, \bar{p}_1 and \bar{p}_2 , have the same sign: from $\bar{p}_2 > 0$ follows $\bar{p}_1 > 0$ and vice versa; from Eq.

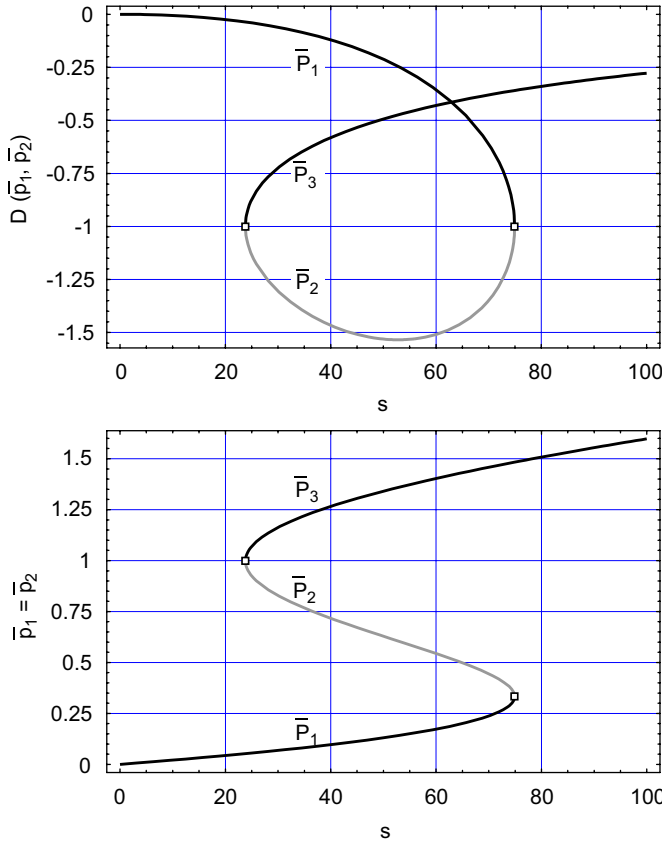


Fig. 7. Position and stability of the three fixed points in the two-gene cooperative activation-activation system with leaky transcription. The influence of basal transcription activity on the bifurcation behavior of the **act-act** system with $n = 2$ is illustrated by variation of γ as in Fig. 5 according to $\gamma_1 = \gamma_2 = 0.001 \cdot s$. The system passes through two saddle-node bifurcations (both marked by \square) at $s = 23.81$ and 74.92 , and it shows hysteresis. The upper part presents $D(\bar{p}_1, \bar{p}_2)$ for the three fixed points as functions of the auxiliary variable s : \bar{P}_1 and \bar{P}_3 are stable, \bar{P}_2 is unstable (stable fixed points: black line; unstable fixed point: gray line). The lower part shows the positions of the three fixed points which lie on the line $p_1 = p_2$ because of the symmetry in the rate constants (coordinates: $\bar{p}_1 = \bar{p}_2$ full line; stability of the fixed point is indicated by black curves, instability by gray curves). Choice of parameters: $k_1^Q = k_2^Q = 2$, $K_1 = K_2 = 1.1$ and $k_1^P = k_2^P = d_1^Q = d_2^Q = d_1^P = d_2^P = 1$.

(33) follows $|\bar{p}_1| > K_1$ for $\bar{p}_1 < 0$ and this leads to $\bar{p}_2 < 0$. Accordingly, one fixed point, \bar{P}_1 , lies inside the negative quadrant of the (p_1, p_2) space, is unstable and plays no role in biology. The second stationary point, \bar{p}_2 , is characterized by two positive concentration values, lies inside the positive quadrant and is stable.

It is straightforward to show that the regulatory determinant never exceeds the value $D = \bar{D}_{\text{Hopf}}$ by applying the same procedure for calculating the limits as in Eqs. (27) and (28). Thereby one obtains for the substitution by auxiliary variables, $k_1^Q = \chi_1 \cdot s$, $k_2^Q = \chi_2 \cdot s$, $K_1 = \lambda_1/s$, $K_2 = \lambda_2/s$, $\vartheta_1 = \delta_1 \cdot s$ and $\vartheta_2 = \delta_2 \cdot s$:

$$\text{limit of large } s: \quad \bar{p}_1 = \alpha_1 \cdot s, \quad \bar{p}_2 = \frac{\lambda_1 \delta_2}{\alpha_1} \cdot \frac{1}{s} \quad \text{with}$$

$$\alpha_1 = \frac{\lambda_1 \delta_2}{2\lambda_2} \left(\sqrt{1 + 4 \frac{\lambda_2 \delta_1}{\lambda_1 \delta_2}} - 1 \right) \quad \text{and}$$

$$\lim_{s \rightarrow \infty} D = D_{\text{lim}} = k_1^P k_2^P \frac{\chi_1 \chi_2 \lambda_1 \lambda_2}{\lambda_1 \delta_2 + \lambda_2 \alpha_1}.$$

The analytical treatment proves that D converges to a finite value D_{lim} whereas \bar{p}_1 diverges and \bar{p}_2 approaches 0 for $s \rightarrow \infty$. It is interesting to note that another choice of s involving only the dissociation constants, $K_1 = \lambda_1/s$, $K_2 = \lambda_2/s$, yields the same result (after replacing χ_1 and χ_2 by k_1^Q and k_2^Q , respectively). To verify $D_{\text{lim}} < \bar{D}_{\text{Hopf}}$ is hard to perform analytically, but easily done numerically. As expected the non-cooperative activation-repression system does not sustain (undamped) oscillations.

Although the fixed point \bar{P}_1 is irrelevant for biology, its properties are, nevertheless, useful for the analysis of the dynamical system in the sense of continuation into the neighboring quadrants. In particular, it allows for an inspection of condition (25). Differentiation shows that the function $D(p_1, p_2)$ of Eq. (21) is always positive and the observation of a Hopf bifurcation cannot be excluded. For the parameter set $k_1^Q = k_2^Q = k_1^P = k_2^P = d_1^Q = d_2^Q = d_1^P = d_2^P = 1$ and $K_1 = K_2 = 1/s$ the regulatory determinant adopts indeed the value $D = \bar{D}_{\text{Hopf}} = 4$ for $s = 2$ at $\bar{P}_1 = (-2, -\frac{1}{3})$. For $s < 2$ the fixed point \bar{P}_1 is unstable and trajectories spiral out of \bar{P}_1 .

In summary, the system shows only the scenario of the unregulated regime for non-negative concentrations, since no bifurcations are observed to states that sustain undamped oscillations or bistability in the positive quadrant. A single stationary state is stable for all values of the physical parameters and, thus, there is no potential for the regulatory properties discussed here.

Cooperative binding: The activation-repression case with $n = 2$ is characterized by a non-negative regulatory determinant ($D \geq 0$), but as discussed in Section 3.2 the maximal value of D is insufficient for a Hopf bifurcation. The system exhibits only one stable fixed point and no undamped oscillations can occur. In other words, the **act-rep** systems with $n = 2$, like the non-cooperative case with $n = 1$, show only an unregulated regime. We remark, however, that other interesting regulatory properties may arise from such negative feedback loops: homeostasis as demonstrated in Tyson et al. (2003) serves as an example.

For $n \geq 3$, however, a Hopf bifurcation is predicted and a limit cycle can be observed for sufficiently strong binding (Figs. 8 and 9). Systems of this class exhibit periodically changing gene activities. Oscillation in regulatory systems can be used as a pacemaker inducing periodicity into metabolism as is observed in circadian and other rhythms. The qualitative picture of the bifurcation diagram is essentially the same for higher Hill coefficients ($n \geq 4$). Along equivalent trajectories leading from the unregulated to the regulated regime the Hopf bifurcation occurs at substantially smaller s values than for $n = 3$. In other words, the regulated domain in parameter space—here the

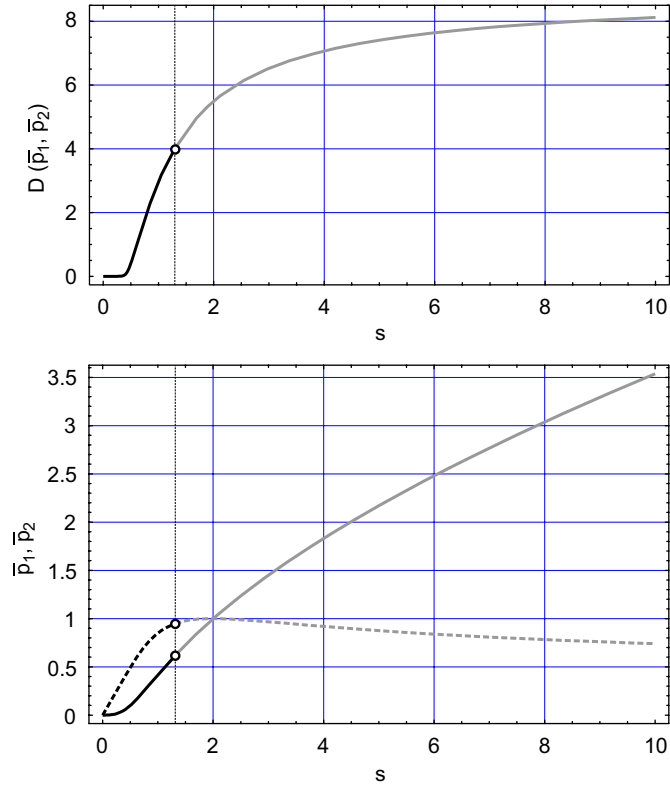


Fig. 8. Position and stability of the fixed point in the two-gene cooperative activation–repression system with Hill coefficient $n = 3$. The upper part of the figure shows the regulatory determinant which is non-negative ($D \geq 0$) as a function of the auxiliary variable s ($k_1^Q = k_2^Q = 2s$, $K_1 = K_2 = 0.5/s$; stable fixed point: black line; unstable fixed point: gray line). D increases with increasing values of s . At $s = 1.2903$ (vertical line in the plots) a Hopf bifurcation (\circ) is observed: the central fixed point becomes unstable and a limit cycle appears (see Fig. 9). The lower part of the figure shows the coordinates of the fixed point (coordinates: \bar{p}_1 full line, \bar{p}_2 broken line; stability of the fixed point is indicated by black curves, instability by gray curves). Choice of other parameters: $k_1^P = k_2^P = d_1^Q = d_2^Q = d_1^P = d_2^P = 1$.

domain that contains an unstable fixed point and a limit cycle—becomes larger with increasing cooperativity as expressed by higher Hill coefficients.

4.3. Repression–repression cases

The binding functions for the repression–repression scenario are

$$F_1(p_2) = \gamma_1 + \frac{K_2}{K_2 + p_2^2} \quad \text{and} \quad F_2(p_1) = \gamma_2 + \frac{K_1}{K_1 + p_1^2}. \quad (34)$$

The discussion of repression–repression cases is organized in two subsections: (i) non-cooperative binding ($\gamma_1 = \gamma_2 = 0$, $n = 1$) and (ii) cooperative binding ($\gamma_1 = \gamma_2 = 0$, $n \geq 2$). Leaky transcription ($\gamma_1 \neq 0, \gamma_2 \neq 0$) will be mentioned later in a comparison of all different regulation scenarios. In the third subsection we compare genetic switches with different Hill coefficients ($n = 2, 3$ and 4).

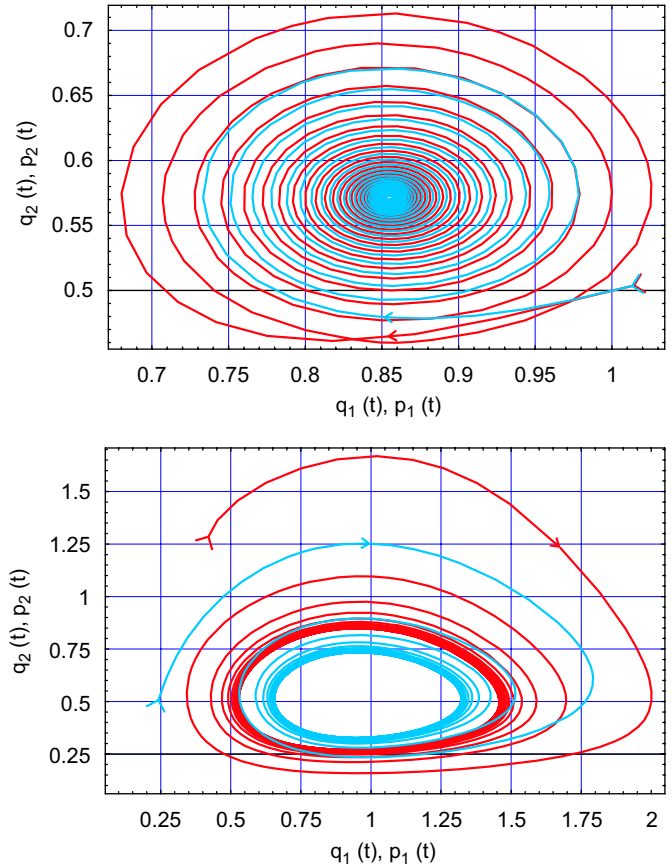


Fig. 9. Stable fixed point and limit cycle in the two-gene cooperative activation–repression system with Hill coefficient $n = 3$. The two plots show trajectories of the system before and after the Hopf bifurcation that occurs at $D(s) = 4$ with $s_{\text{Hopf}} = 2.17$ in the system with $k_1^Q = k_2^Q = 1 \cdot s$ and $K_1 = K_2 = 0.5/s$ and $k_1^P = k_2^P = d_1^Q = d_2^Q = d_1^P = d_2^P = 1$. The upper plot shows a trajectory for $s = 2$ ($D(2) = 3.6804$) with a stable fixed point and the trajectories spiralling inwards, the lower plot was recorded for $s = 2.5$ ($D(2.5) = 4.5265$) where the fixed point is unstable and a stable limit cycle is observed. The trajectories spiral from outside towards the limit cycle. For initial conditions near the unstable fixed point the limit cycle is approached through spiralling outwards (not shown). Color code: The projection of the trajectory onto the mRNA concentration subspace, $(q_1(t), q_2(t))$, is shown in red and the projection onto the protein subspace, $(p_1(t), p_2(t))$, is plotted in blue.

Non-cooperative binding: Again, two stationary solutions are obtained as solutions of a quadratic equation

$$K_2 \bar{p}_1^2 + (\vartheta_2 K_1 - \vartheta_1 K_2 + K_1 K_2) \bar{p}_1 - \vartheta_1 K_1 K_2 = 0,$$

and the same relation as in the previous section:

$$\bar{p}_2 = \frac{\vartheta_2 K_1}{K_1 + \bar{p}_1}.$$

As in the previous example it can be proven that \bar{p}_1 and \bar{p}_2 always have the same sign at both fixed points. One of the two solutions is unstable and lies in the negative quadrant whereas the other one, the physically meaningful solution, is situated in the positive quadrant and it is asymptotically stable. The observed stabilities are readily predicted from inspection of Eq. (21): since D is non-positive we have either four real negative eigenvalues or two real eigenvalues

and a complex conjugate pair with a real part lying between the other two (Fig. 2). The stable fixed point is identified by $0 \geq D \geq -1$, the unstable one by $D < -1$.

In the non-cooperative binding case the repression–repression combination gives rise to only one stable state corresponding to the unregulated scenario. Hence, it is not suitable for regulation.

Cooperative binding: The cooperative repression–repression system is the prototype of a genetic switch. At low affinities the system sustains one asymptotically stable stationary state. In the regulated regime it shows bistability consisting of two asymptotically stable states that can be characterized as \mathbf{G}_1 active and \mathbf{G}_2 silenced and vice versa, \mathbf{G}_2 active and \mathbf{G}_1 silenced. The two states are separated by a saddle point (\bar{P}_1 in Fig. 10 and \bar{P}_4 in Fig. 12, respectively). For symmetric choices of parameters, implying that all parameters for \mathbf{G}_1 have values identical to those of the corresponding parameters for \mathbf{G}_2 , a pitchfork bifurcation separates the unregulated regime from the regulated regime (Fig. 10). The fixed point \bar{P}_1 becomes unstable and two new fixed points, \bar{P}_2 and \bar{P}_3 , corresponding to two regulatory states emerge. Both are stable and they occur at mirror symmetric positions relative to the line $p_1 = p_2$ bisecting the positive quadrant: $\bar{P}_2 = (a, b)$ and $\bar{P}_3 = (b, a)$ with $a > b$. At \bar{P}_2 \mathbf{G}_1 shows higher activity than \mathbf{G}_2 , and at \bar{P}_3 the situation is inverse, \mathbf{G}_2 shows higher activity than \mathbf{G}_1 . Considering identical paths through parameter space the position of the pitchfork bifurcation is shifted towards smaller values of the auxiliary parameter s in the series $n = 2, 3, 4$ (Table 2). Apart from this difference the bifurcation patterns are remarkably similar in the parametric plot shown in Fig. 11.

Introducing asymmetry through different values for k_1^Q and k_2^Q and/or K_1 and K_2 , respectively, removes the degeneracy and converts the pitchfork into a saddle-node bifurcation (Figs. 12 and 13). The fixed point of the unregulated regime (\bar{P}_1) is transformed continuously into one of the two regulatory states. In particular, this is the state that has the higher rate constant k^Q and/or the smaller complex dissociation constant K (\bar{P}_3 in the figure). The second regulatory state, the one which is characterized by the smaller k^Q and/or the larger K value (\bar{P}_2 in the figure), is created together with the saddle point at the bifurcation. As illustrated nicely by the parametric plots in the middle and at the bottom of Fig. 12, the stable fixed point of the unregulated regime is attracted towards the (no longer extant) pitchfork bifurcation. Such a phenomenon is often called the influence of a ‘ghost’ on bifurcation lines or trajectories. The transition from the saddle-node to the pitchfork bifurcation is seen best in the plots of the fixed point positions as functions of the auxiliary parameter s shown in Fig. 13: the diagram converges smoothly towards the ‘pitchfork’ in the symmetric case (Fig. 10).

Genetic switches with different Hill coefficients: The regulatory properties of repression–repression systems are of primary interest in computations of genabolic networks because of their switching potential. As said above, the

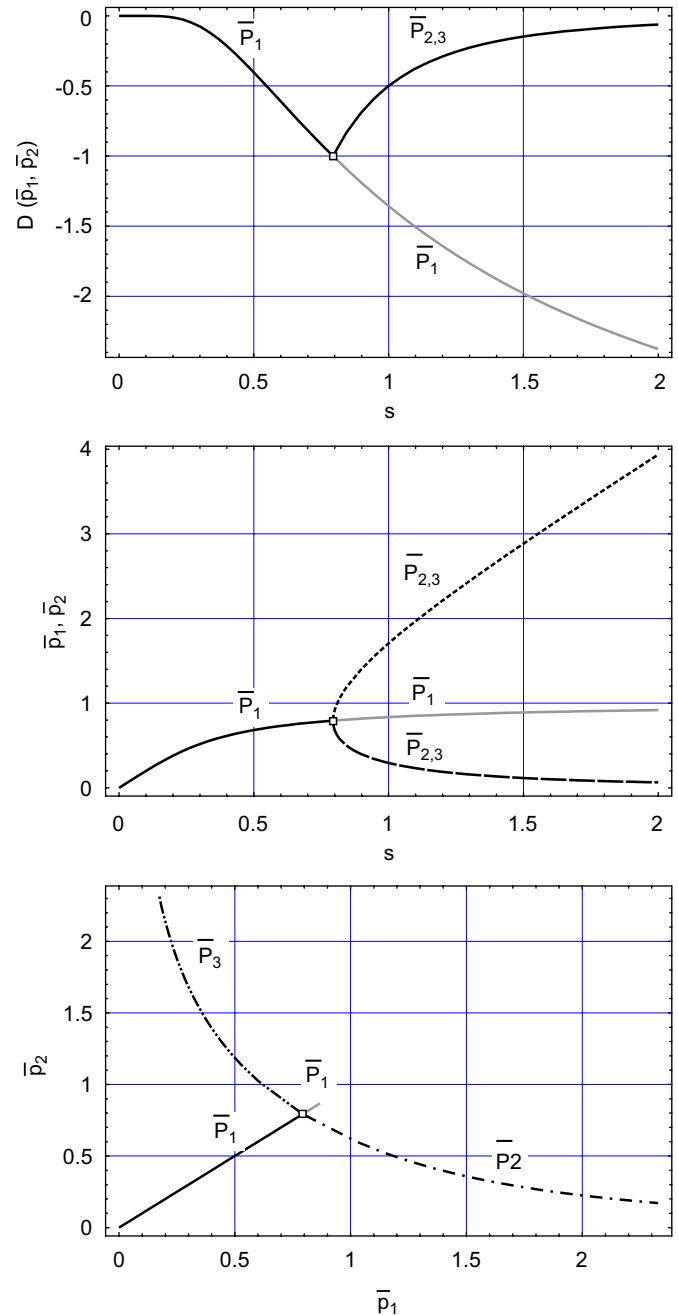


Fig. 10. Position and stability of the fixed points in the symmetric two-gene cooperative repression–repression system with $n = 2$. The one-dimensional bifurcation is a pitchfork (marked by \square) at the value $s = 0.7937$ for the following choice of parameters: $k_1^Q = k_2^Q = 2 \cdot s$, $K_1 = K_2 = 0.5/s$ and $k_1^P = k_2^P = d_1^Q = d_2^Q = d_1^P = d_2^P = 1$. The topmost plot shows the dependence of the regulatory determinants on s (because of symmetry the values of D at \bar{P}_2 and \bar{P}_3 are identical; stable fixed points: black line; unstable fixed point: gray line). In the middle we present the positions of the fixed points as function of s (coordinates: $\bar{P}_1(\bar{p}_1 = \bar{p}_2)$ full line; stability of the fixed point is indicated by the black curve, instability by the gray curve; the two broken lines show the coordinates of the other two fixed points \bar{P}_2 and \bar{P}_3). The figure at the bottom presents a parametric plot of the positions of all fixed points, $\bar{P}_k = (\bar{p}_1^{(k)}(s), \bar{p}_2^{(k)}(s))$ (stable points: black lines full and broken, unstable point: gray line).

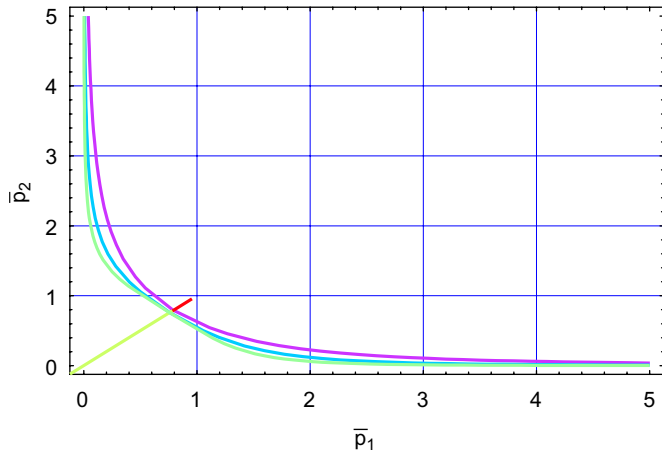


Fig. 11. Position of fixed points in the two-gene cooperative repression-repression system. The parametric plot shows a superposition of the pitchfork diagrams for the Hill coefficients $n = 2, 3$ and 4 with the varied parameters $k_1^Q = k_2^Q = 2 \cdot s$ and $K_1 = K_2 = 0.5/s$ defining the path through parameter space. Choice of the other parameters: $k_1^P = k_2^P = d_1^Q = d_2^Q = d_1^P = d_2^P = 1$. Color code: Chartreuse: stable regime of fixed point \bar{P}_1 ; red: unstable regime of fixed point \bar{P}_1 ; violet: fixed points $\bar{P}_{2,3}$ with $n = 2$; blue: fixed points $\bar{P}_{2,3}$ with $n = 3$; green: fixed points $\bar{P}_{2,3}$ with $n = 4$.

value of s at the pitchfork or saddle-node bifurcation decreases substantially for increasing Hill coefficients (Table 2). Two more properties are highly relevant in the context of regulation: (i) the ‘pitchforks’ in parametric plots for different Hill coefficients are surprisingly similar (Fig. 11) and (ii) the regulatory selectivity increases strongly in the sequence $n = 2, 3$ and 4 (Table 3).

The superposition of the three pitchfork diagrams in Fig. 11 reveals astonishing agreements of the plots for three different Hill coefficients ($n = 2, 3, 4$). This general behavior is changed slightly only when different paths through parameter space are chosen as long as the kinetic parameters are scaled by $k_1^Q = \chi_1 \cdot s$ and $k_2^Q = \chi_2 \cdot s$. Constant values of K_1 and K_2 , for example, have little influence on the diagram. If the dissociation constants, however, are varied, for example, $K_1 = \lambda_1/s$ and $K_2 = \lambda_2/s$, and two kinetic parameters are chosen to be constant, the bifurcation diagram changes shape substantially. The differences in the plots are explained readily by inspection of the limits derived for the paths through parameter space. As an example we present the limits of the fixed points for the two cases mentioned above (see also Table 1):

$$\begin{aligned} \vartheta_1 &= \delta_1 \cdot s, \vartheta_2 = \delta_2 \cdot s, K_1, K_2: \\ \lim_{s \rightarrow 0} \bar{P}_1 &= (0, 0), \lim_{s \rightarrow \infty} \bar{P}_1 = (\infty, \infty), \\ \lim_{s \rightarrow \infty} \bar{P}_2 &= (\infty, 0), \lim_{s \rightarrow \infty} \bar{P}_3 = (0, \infty), \\ \vartheta_1, \vartheta_2, K_1 = \lambda_1/s, K_2 = \lambda_2/s: \\ \lim_{s \rightarrow 0} \bar{P}_1 &= (\vartheta_1, \vartheta_2), \lim_{s \rightarrow \infty} \bar{P}_1 = (0, 0), \\ \lim_{s \rightarrow \infty} \bar{P}_2 &= (\vartheta_1, 0), \lim_{s \rightarrow \infty} \bar{P}_3 = (0, \vartheta_2). \end{aligned}$$

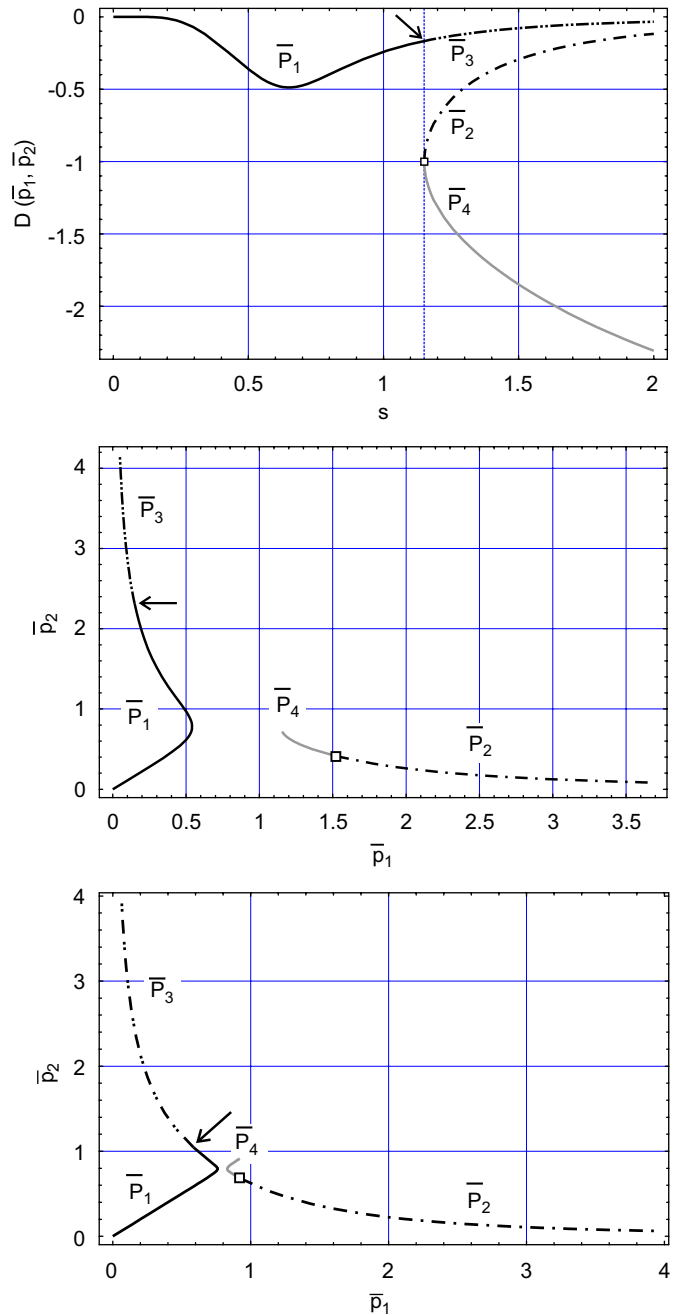


Fig. 12. Position and stability of the fixed points in the asymmetric two-gene cooperative repression-repression system with $n = 2$. The pitchfork bifurcation of the symmetric case (Fig. 10) is replaced by a saddle-node bifurcation (marked by \square) that occurs here at $s_{\text{oneD}} = 1.1515$ for the parameter choice: $k_1^Q = 1.9 \cdot s, k_2^Q = 2.1 \cdot s, K_1 = 0.55/s, K_2 = 0.45/s$ and $k_1^P = k_2^P = d_1^Q = d_2^Q = d_1^P = d_2^P = 1$. The topmost plot shows the dependence of the regulatory determinant D on s (stable fixed points: black line; unstable fixed point: gray line). The distinction between \bar{P}_1 and \bar{P}_3 is made for illustration, they represent the same fixed point at different ranges of s . The position of $\bar{P}_1 \equiv \bar{P}_3$ at $s = 1.1515$ is marked by the arrow. In the middle we present the corresponding parametric plot of the positions of all fixed points, $\bar{P}_k = (\bar{p}_1^{(k)}(s), \bar{p}_2^{(k)}(s))$ (stable points: black lines full and broken, unstable point: gray line). The plot at the bottom differs from the middle plot in the choice of parameters: $k_1^Q = 1.999 \cdot s, k_2^Q = 2.001 \cdot s, K_1 = 0.501/s, K_2 = 0.499/s$; the bifurcation occurs at $s_{\text{oneD}} = 0.8105$ (\leftarrow).

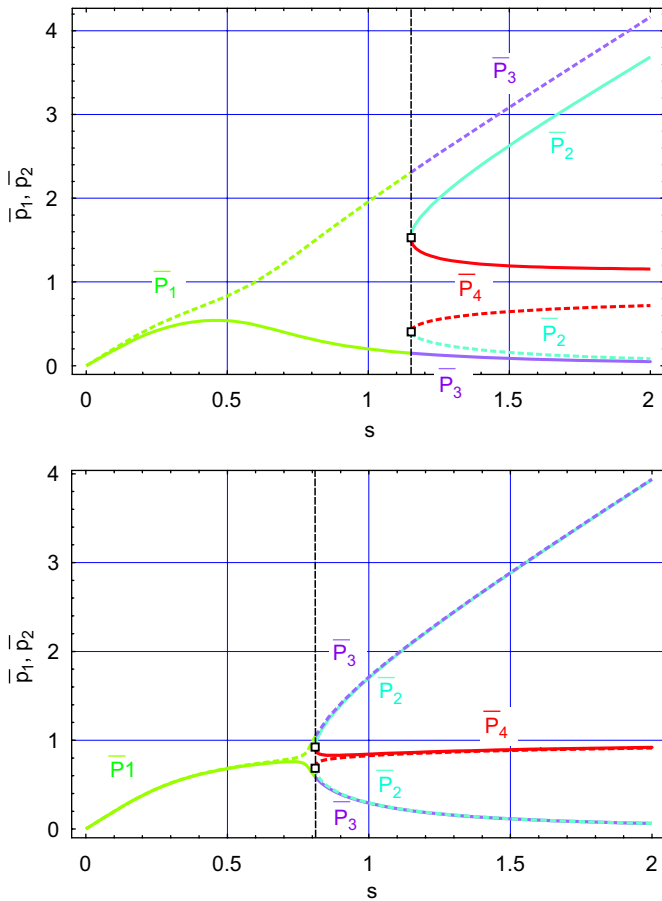


Fig. 13. The transition from saddle node to pitchfork bifurcation in the asymmetric two-gene cooperative repression–repression system with $n = 2$. The coordinates of fixed points are given as functions of the auxiliary parameter s . The choice of the constant parameters is the same as in Fig. 12, $k_1^P = k_2^P = d_1^Q = d_2^Q = d_1^P = d_2^P = 1$ and $k_1^Q = 1.9 \cdot s$, $k_2^Q = 2.1 \cdot s$, $K_1 = 5/s$, $K_2 = 0.45/s$ (upper plot) or $k_1^Q = 1.999 \cdot s$, $k_2^Q = 2.001 \cdot s$, $K_1 = 0.501/s$, $K_2 = 0.499/s$ (lower plot), as is the notation of fixed points \bar{P}_k , $k = 1, \dots, 4$. In particular, \bar{P}_1 and \bar{P}_3 are the same fixed point at s values before and after the saddle-node bifurcation. The coordinates of fixed points $\bar{p}_1^{(k)}(s)$ and $\bar{p}_2^{(k)}(s)$ are shown as full and broken lines, respectively. The pitchfork bifurcation of the symmetric case (Fig. 10) is replaced by a saddle-node bifurcation (marked by \square) that occurs here at $s = 1.1515$ (upper plot) and $s = 0.8105$ (lower plot). The lower plot is suggestive for the transition between the two bifurcation types: as $(k_1^Q - k_2^Q) \rightarrow 0$ and $(K_1 - K_2) \rightarrow 0$ the two coordinates of the fixed points \bar{P}_1 and \bar{P}_4 approach each other and the points converge to positions on the line $p_1 = p_2$, whereas the opposite coordinates become pairwise identical for \bar{P}_2 and \bar{P}_3 , $(\bar{p}_1^{(2)} - \bar{p}_2^{(3)}) \rightarrow 0$ and $(\bar{p}_1^{(3)} - \bar{p}_2^{(2)}) \rightarrow 0$. Accordingly the two stable fixed points occupy symmetric positions with respect to $p_1 = p_2$. Color code: Chartreuse: stable fixed point $\bar{P}_1 (= \bar{P}_3)$; turquoise: stable fixed point \bar{P}_2 ; violet: stable fixed point $\bar{P}_3 (= \bar{P}_1)$; red: unstable fixed point \bar{P}_4 .

Simultaneous variation of the ϑ parameters and the equilibrium constants K results in the same behavior as variation of the former parameters alone. Clearly, only patterns with the same limits are comparable and in the current example we chose the former case, variation of kinetic parameters with or without variation of dissociation constants.

In Table 3 the efficiency of genetic switches is compared for different Hill coefficients. The numbers illustrate the effect of higher order cooperativity: the higher the value of n , the larger is the selective power of the switch. At $s = 4$, for example, we find the mole fractions¹⁰ $\bar{x}_2 = 0.067$, 0.030 and 0.015 for the protein of the silenced gene for the Hill coefficients $n = 2, 3$ and 4 , respectively. Since the pitchfork diagrams are not very different for the three cases the efficiency in silencing is caused by the different values of s at comparable points. An illustration of this argument is given by the bifurcation point itself which occurs at $s = 1, 0.211$ and 0.069 for $n = 2, 3$ and 4 , respectively.

Summary: Cooperative repression–repression systems are recognized for their importance as genetic switches. Hill coefficients higher than $n = 2$ have two properties that are relevant for regulation: (i) the regulated regime comprises a larger domain in parameter space and (ii) the selectivity of the regulatory function increases with increasing n .

4.4. Influence of basal transcription on bifurcation patterns

The influence of basal transcription on all three classes of regulatory systems (**act–act**, **act–rep** and **rep–rep**) is compared in Fig. 14. For simplicity the diagrams show only the symmetric cases, $\gamma_1 = \gamma_2 = \gamma$ and $\vartheta_1 = \vartheta_2 = \vartheta$, and the systems with the lowest values of the Hill coefficient at which the characteristic bifurcation pattern appears ($n = 2$ for **act–act** and **rep–rep**, and $n = 3$ for **act–rep**). All three systems have in common that the bifurcations vanish at sufficiently large values of $\gamma > \gamma_{crit}$ and then the systems sustain only one stable state. Below γ_{crit} we find the specific bifurcation pattern for the systems in a certain range $\vartheta_{crit}^{(1)} < \vartheta < \vartheta_{crit}^{(2)}$: the bifurcation at low values of ϑ is compensated by an inverse bifurcation of the same class at higher ϑ values. For all systems the inverse bifurcation point approaches infinity for vanishing basal transcription: $\lim_{\gamma \rightarrow 0} \vartheta_{crit}^{(2)} = +\infty$. There is, however, one characteristic difference between the three bifurcation diagrams: the lower bifurcation line has a negative slope in the **act–act** system but a positive slope in the two other classes, **act–rep** and **rep–rep**. This implies that for increasing basal transcription $\gamma < \gamma_{crit}$ the saddle-node bifurcation occurs at lower values of ϑ , whereas increasing basal activity drives the first bifurcation to higher ϑ values in the other two classes of systems.

4.5. Two examples of intermediate regulation

In order to illustrate the bifurcation pattern with respect to regulatory determinants D that can change sign we consider two examples of regulation by intermediate complexes: (i) a combination of activation and intermediate regulation and (ii) a combination of repression and

¹⁰The mole fractions are defined by $\bar{x}_1 = \bar{p}_1 / (\bar{p}_1 + \bar{p}_2)$ and $\bar{x}_2 = \bar{p}_2 / (\bar{p}_1 + \bar{p}_2)$.

Table 3

Position of the bifurcation point in repression–repression systems and switching efficiency for different Hill coefficients $n = 2, 3, 4$

n	Variable s at bifurcation	Position $\bar{p}_1 = \bar{p}_2$	Silencing efficiency ^a		
			$s = 1.5$	$s = 2.5$	$s = 4.0$
2	1	1	(1.577, 0.423)	(1.775, 0.225)	(1.866, 0.134)
3	0.2109	1.333	(1.989, 0.156)	(1.996, 0.096)	(1.998, 0.061)
4	0.0685	1.500	(2.000, 0.080)	(2.000, 0.049)	(2.000, 0.031)

The values in the table are sampled on equivalent paths through parameter space with the following parameter values: $k_1^Q = k_2^Q = 2$, $K_1 = K_2 = 1/s$ and $k_1^P = k_2^P = d_1^Q = d_2^Q = d_1^P = d_2^P = 1$. Because of symmetry the bifurcation is of pitchfork type.

^aThe values in parentheses represent the stationary concentrations of regulator proteins, (\bar{p}_1, \bar{p}_2) , at the fixed point \bar{P}_1 for the given value of the auxiliary variable s .

intermediate regulation. Both cases have a Hill coefficient $n = 4$. The four complexes formed by successive binding are shown together with the various forms of potential transcriptional regulation in Fig. 15. The four dissociation constants are multiplied to yield the following combinations:

$$\begin{aligned} \kappa_{11} &= K_{11} \cdot K_{12} \cdot K_{13} \cdot K_{14}, & \kappa_{12} &= K_{12} \cdot K_{13} \cdot K_{14}, \\ \kappa_{13} &= K_{13} \cdot K_{14}, & \kappa_{14} &= K_{14}, \\ \kappa_{21} &= K_{21} \cdot K_{22} \cdot K_{23} \cdot K_{24}, & \kappa_{22} &= K_{22} \cdot K_{23} \cdot K_{24}, \\ \kappa_{23} &= K_{23} \cdot K_{24}, & \kappa_{24} &= K_{24}. \end{aligned}$$

As mentioned in Section 2.1 the equilibrium parameters used here are macroscopic dissociation constants.

In the first system the saturated complex $\mathbf{H}_1^{(4)}$ ($F_1(\bar{p}_2)$) and the ‘intermediate 2’ $\mathbf{H}_2^{(2)}$ ($F_2(\bar{p}_1)$) initiate transcription and the binding functions are of the form

$$F_1(\bar{p}_2) = \frac{\bar{p}_2^4}{\kappa_{21} + \kappa_{22}\bar{p}_2 + \kappa_{23}\bar{p}_2^2 + \kappa_{24}\bar{p}_2^3 + \bar{p}_2^4} \quad \text{and}$$

$$F_2(\bar{p}_1) = \frac{\kappa_{13}\bar{p}_1^2}{\kappa_{11} + \kappa_{12}\bar{p}_2 + \kappa_{13}\bar{p}_1^2 + \kappa_{14}\bar{p}_1^3 + \bar{p}_1^4}.$$

Computation of the regulatory determinant D is straightforward and yields

$$D(\bar{p}_1, \bar{p}_2) = -k_1^Q k_2^Q k_1^P k_2^P \times \frac{\kappa_{13}\bar{p}_1\bar{p}_2^3(2\kappa_{11} + \kappa_{12}\bar{p}_1 - \kappa_{14}\bar{p}_1^3 - 2\bar{p}_1^4)(4\kappa_{21} + 3\kappa_{22}\bar{p}_2 + 2\kappa_{23}\bar{p}_2^2 + \kappa_{24}\bar{p}_2^3)}{(\kappa_{11} + \kappa_{12}\bar{p}_2 + \kappa_{13}\bar{p}_1^2 + \kappa_{14}\bar{p}_1^3 + \bar{p}_1^4)^2(\kappa_{21} + \kappa_{22}\bar{p}_2 + \kappa_{23}\bar{p}_2^2 + \kappa_{24}\bar{p}_2^3 + \bar{p}_2^4)^2}.$$

bifurcation of **act–act** systems. The system sustains one or three stationary states. The state at the origin is always stable. Then it passes through two bifurcations as a function of the auxiliary variable s . The first of them is a saddle-node bifurcation at $s = s_{\text{oneD}}$, which is found in all cooperative activation–activation systems. The bifurcation gives birth to one stable and one unstable state. The new stable state moves outwards in the positive quadrant, i.e. to larger values of \bar{p}_1 and \bar{p}_2 , and the unstable state moves inwards. As shown in Fig. 16 the system indeed passes a Hopf bifurcation at $s = s_{\text{Hopf}}$ and a stable limit cycle is formed.

The second example of intermediate regulation combines repression ($F_1(\bar{p}_2)$) and an active intermediate complex ($F_2(\bar{p}_1)$). Here \mathbf{G}_1 and the ‘intermediate 2’ $\mathbf{H}_2^{(2)}$ are the active transcription forms. The two regulatory functions are given by

$$F_1(\bar{p}_2) = \frac{\kappa_{21}}{\kappa_{21} + \kappa_{22}\bar{p}_2 + \kappa_{23}\bar{p}_2^2 + \kappa_{24}\bar{p}_2^3 + \bar{p}_2^4} \quad \text{and}$$

$$F_2(\bar{p}_1) = \frac{\kappa_{13}\bar{p}_1^2}{\kappa_{11} + \kappa_{12}\bar{p}_2 + \kappa_{13}\bar{p}_1^2 + \kappa_{14}\bar{p}_1^3 + \bar{p}_1^4}.$$

Computation of the regulatory determinant D now yields

$$D(\bar{p}_1, \bar{p}_2) = k_1^Q k_2^Q k_1^P k_2^P \times \frac{\kappa_{13}\kappa_{21}\bar{p}_1(2\kappa_{11} + \kappa_{12}\bar{p}_1 - \kappa_{14}\bar{p}_1^3 - 2\bar{p}_1^4)(\kappa_{22} + 2\kappa_{23}\bar{p}_2 + 3\kappa_{24}\bar{p}_2^2 + 4\bar{p}_2^3)}{(\kappa_{11} + \kappa_{12}\bar{p}_2 + \kappa_{13}\bar{p}_1^2 + \kappa_{14}\bar{p}_1^3 + \bar{p}_1^4)^2(\kappa_{21} + \kappa_{22}\bar{p}_2 + \kappa_{23}\bar{p}_2^2 + \kappa_{24}\bar{p}_2^3 + \bar{p}_2^4)^2}.$$

In principle, D can adopt plus and minus signs and a Hopf bifurcation may occur in addition to the one-dimensional

Again, plus and minus signs are possible and as documented in Fig. 17 two bifurcations, the pitchfork bifurcation

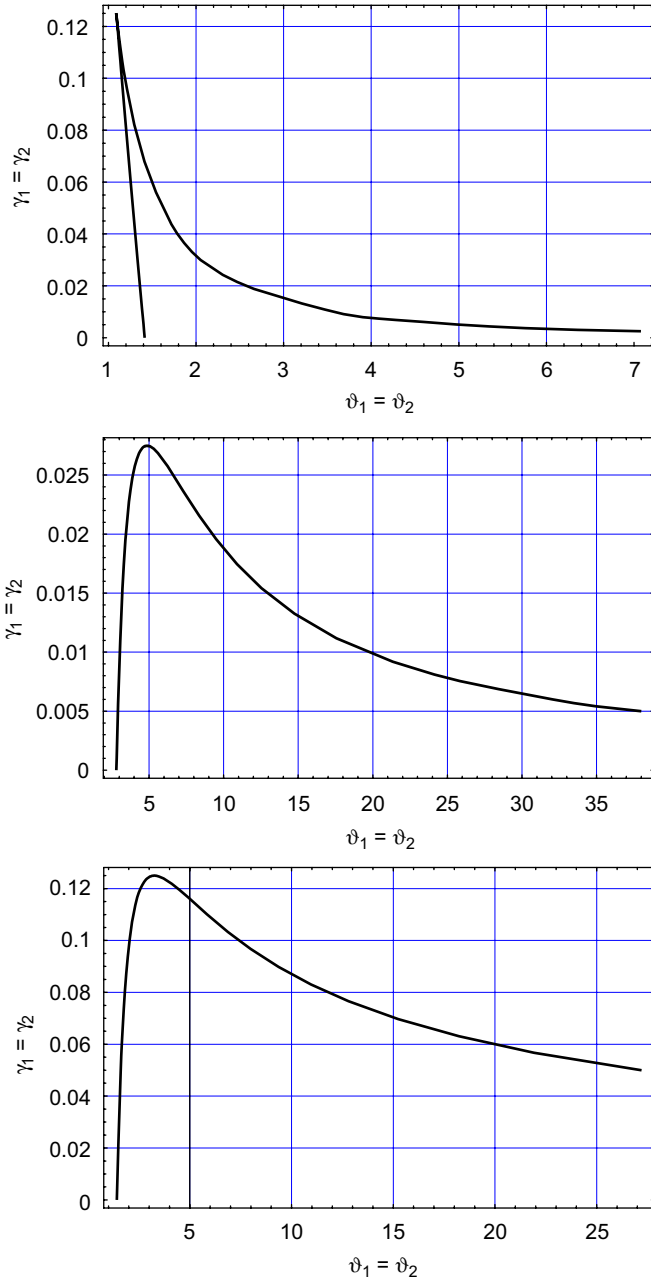


Fig. 14. The influence of basal transcription on the bifurcation patterns of gene regulation. The topmost plot presents the positions of the saddle-node bifurcations of the **act-act** system with Hill coefficient $n = 2$ in the (ϑ, γ) plane. In the area enclosed by the curves we observe three stationary states, elsewhere one stable stationary state. The plot in the middle refers to the **act-rep** system with Hill coefficient $n = 3$: oscillations occur below the bifurcation curve. The plot at the bottom shows the analogous curve of the **rep-rep** system with Hill coefficient $n = 2$. Three steady states are observed between two (opposite) pitchfork bifurcations, i.e. in the area below the curve. Other parameters: $K_1 = K_2 = 0.5$, and $k_1^Q = \vartheta_1 = k_2^Q = \vartheta_2$, $k_1^P = k_2^P = d_1^Q = d_2^Q = d_1^P = d_2^P = 1$ for the middle plot.

which is typical for cooperative **rep-rep** systems and a Hopf bifurcation, are indeed observed.

Without showing details we mention that the Hopf bifurcation was not observed for all systems with

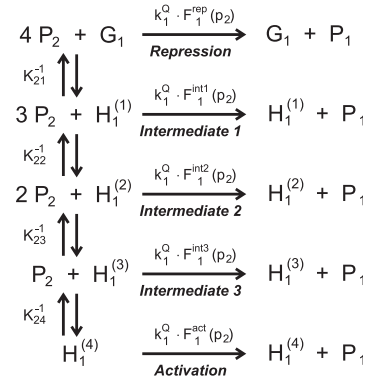


Fig. 15. Intermediate complexes as active forms in transcription. A four-step binding equilibrium of four monomers to a binding site in the gene regulatory region is shown as an example for the dynamics of regulation by means of active intermediate complexes. Three intermediate complexes, $H_1^{(1)}$, $H_1^{(2)}$ and $H_1^{(3)}$, are potential candidates for transcription.

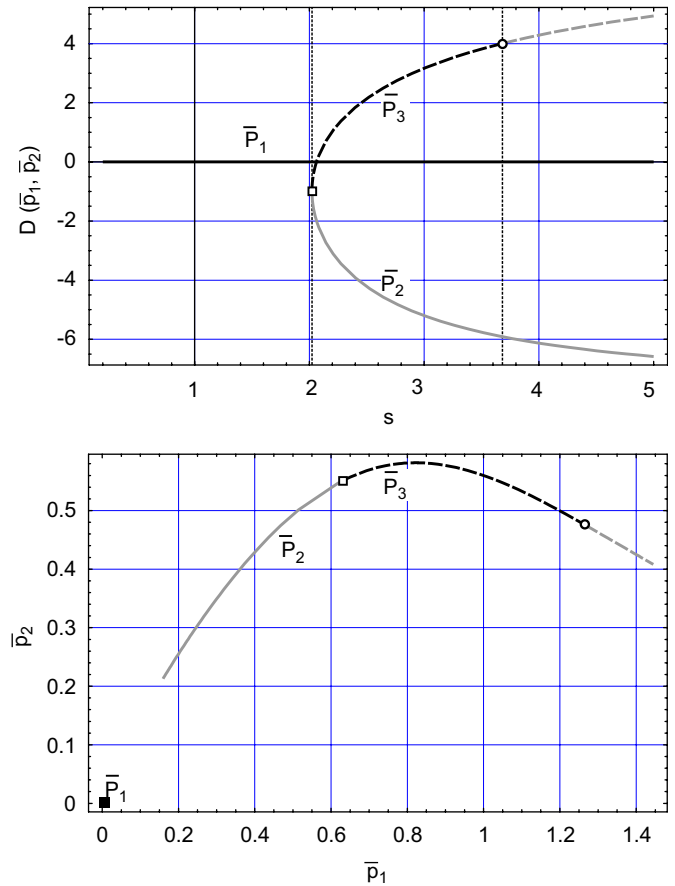


Fig. 16. Position and stability of the three fixed points in the two-gene cooperative system with intermediate activation and a Hill coefficient of $n = 4$. The active entities are $H_1^{(4)}$ and $H_2^{(2)}$. A saddle-node bifurcation (\square) and a Hopf bifurcation (\circ) are observed at $s = 2.023$ and 3.671 , respectively. Choice of parameters: $k_1^Q = k_2^Q = 2 \cdot s$, $\kappa_{11} = \kappa_{12} = \dots = \kappa_{24} = 0.5/s$ and $k_1^P = k_2^P = d_1^Q = d_2^Q = d_1^P = d_2^P = 1$. The upper plot shows D as a function of the auxiliary variable s (stable fixed points: black lines; unstable fixed points: gray lines). The lower plot is a parametric plot of the positions of all fixed points as functions of s : $P_k = (p_1^{(k)}(s), p_2^{(k)}(s))$, $k = 1, 2, 3$ (stable fixed points: full and broken black lines; unstable fixed points: full and broken gray lines).

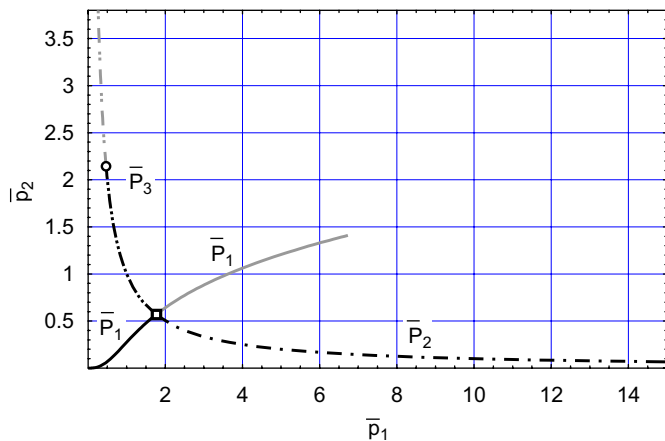


Fig. 17. Position and stability of the three fixed points in the two-gene cooperative system with intermediate repression and Hill coefficient $n = 4$. The active entities are \mathbf{G}_1 and $\mathbf{H}_2^{(2)}$. A pitchfork bifurcation (\square) and a Hopf bifurcation (\circ) are observed at $s = 3.834$ and 17.96 , respectively. Choice of parameters: $k_1^Q = k_2^Q = 1 \cdot s$, $\kappa_{11} = \kappa_{12} = \dots = \kappa_{24} = 1$ and $k_1^P = k_2^P = d_1^Q = d_2^Q = d_1^P = d_2^P = 1$. The plot shows the positions of all fixed points as functions of s : $\bar{P}_k = (\bar{p}_1^{(k)}(s), \bar{p}_2^{(k)}(s))$, $k = 1, 2, 3$ (stable fixed points: full and broken black lines; unstable fixed points: full and broken gray lines).

regulatory determinants D that can have plus or minus sign. For example, no oscillations are observed in the systems transcribing $\mathbf{H}_2^{(4)}$ and ‘intermediate 1’ $\mathbf{H}_2^{(1)}$ or \mathbf{G}_1 and ‘intermediate 1’ $\mathbf{H}_2^{(1)}$, respectively. More examples are listed in Table 5. The situation in these cases is analogous to the activation–repression system with Hill coefficient $n = 2$: the regulatory determinant D adopts positive values but does not exceed $D = D_{\text{Hopf}}$ for all tested values and approached limits.

5. Numerical sampling of parameter space

The results derived from selected examples are summarized and augmented by numerical explorations of parameter space in this section. Numerical sampling was performed in an explorative manner in order to learn whether or not more complicated cases exist where the computer assisted analytic approach applied here is doomed to fail. For the sampling approach we assumed a constant total gene concentration of $g_0 = 1$ in suitable arbitrary units (see Section 6). All rate and equilibrium parameters, π_k , $k = 1, 2, \dots$, were allowed to adopt values in the range $-9.25 \leq \log \pi_k \leq 9.25$ corresponding to approximately $10^{-4} \leq \pi_k \leq 10^4$. Individual values were sampled by means of a random number generator assuming uniform distribution on the logarithmic scale. A typical sample consisted of some ten thousand points and the distribution of different dynamical behaviors was evaluated by simple frequency counting. The results are summarized in Tables 4 and 5. Despite relatively small samples all qualitative forms of dynamic behavior were detected by the numerical sampling procedure.

Table 4 also presents an overview of all activation and repression cases with simple Hill-type functions (5) for $n = 1, 2, 3$ and 4. Basal activation or leaky transcription were also included. Almost all systems under consideration show an unregulated and a regulated regime separated by a bifurcation. The only exceptions are non-cooperative systems and the **act–rep** system with Hill coefficient $n = 2$.

Not all intermediate cases were investigated but the examples shown in Table 5 are representative. They show transitions from behavior characteristic of one basic regulatory combination to another, for example, from **act–rep** to **act–act** in the table. The pure combinations have their well-defined characteristic behavior, Hopf bifurcation and undamped oscillations for **act–rep** and one-dimensional bifurcation and bistability for **act–act** and **rep–rep**. The intermediate cases form a smooth transition in the sense that they combine both scenarios, first one-dimensional bifurcation and second Hopf bifurcation (one example combining both scenarios is shown in Fig. 16). The best studied and documented example is the case for Hill coefficient $n = 4$ in the table. All five objects from the naked gene to the complex with four monomers bound to DNA that can possibly initiate transcription are considered in the table. The pure systems show oscillations or bistability (with one state being the origin) and the intermediate complexes combine both behaviors—‘intermediate 1’ and ‘intermediate 2’—or they behave like the **act–act** system—‘intermediate 3’.

A very similar situation is encountered for the repression–intermediate system. We cannot give the details here, but Fig. 17 shows a parametric plot for one intermediate case, \mathbf{G}_1 and $\mathbf{H}_2^{(2)}$, that exhibits both, a one-dimensional bifurcation leading to bistability with one state having one gene active and the other one silenced and the second state vice versa. Later, with increasing ϑ/K ratios one state becomes unstable and gives birth to a stable limit cycle via a Hopf bifurcation.

6. Discussion

The work reported here aims at the presentation of a straightforward and fairly simple mathematical technique that allows for full characterization of the dynamical patterns for gene regulation by transcription kinetics following Eqs. (11) and (12). The procedure can be extended to investigations of the entire parameter space since, despite a rather large number of kinetic parameters and equilibrium binding constants, only very few quantities determine the dynamical pattern of the system—as encapsulated in the fixed points and their stabilities: stationary mRNA concentrations (15) are proportional to stationary protein concentrations (14) and therefore it is sufficient to study the dynamical systems in the protein subspace. Moreover, the fixed points in protein space depend only on the binding function and one rational expression of kinetic parameters, $\vartheta_j = (k_j^Q k_j^P)/(d_j^Q d_j^P)$, for

Table 4
Results of bifurcation analysis of systems with simple binding functions (5) for activation and repression

Regulation G_1		Regulation G_2		Dynamical pattern ^a	Number of non-negative roots ^b	Bifurcation type
Type	$F_1(p_2)$	Type	$F_2(p_1)$			
Activation	$\frac{p_2}{K_2 + p_2}$	Activation	$\frac{p_1}{K_1 + p_1}$	$E S$	1 2 (2)	Transcritical
Activation	$\frac{p_2}{K_2 + p_2}$	Repression	$\frac{p_1}{K_1 + p_1}$	S	1 (2)	
Repression	$\frac{K_2}{K_2 + p_2}$	Repression	$\frac{K_2}{K_1 + p_1}$	S	1 (2)	
Activation	$\frac{p_2^2}{K_2 + p_2^2}$	Activation	$\frac{p_1^2}{K_1 + p_1^2}$	$E B(E, S)$	1 3 (5)	Saddle-node
Activation	$\frac{p_2^2}{K_2 + p_2^2}$	Repression	$\frac{K_1}{K_1 + p_1^2}$	S	1 (5)	
Repression	$\frac{K_2}{K_2 + p_2^2}$	Repression	$\frac{K_1}{K_1 + p_1^2}$	$S B(S_1, S_2)$	1 3 (5)	Pitchfork or saddle-node
Activation	$\frac{p_2^3}{K_2 + p_2^3}$	Activation	$\frac{p_1^3}{K_1 + p_1^3}$	$E B(E, S)$	1 3 (9)	Saddle-node
Activation	$\frac{p_2^3}{K_2 + p_2^3}$	Repression	$\frac{K_1}{K_1 + p_1^3}$	$S O$	1 1 (9)	Hopf
Repression	$\frac{K_2}{K_2 + p_2^3}$	Repression	$\frac{K_1}{K_1 + p_1^3}$	$S B(S_1, S_2)$	1 3 (9)	Pitchfork or saddle-node
Activation	$\frac{p_2^4}{K_2 + p_2^4}$	Activation	$\frac{p_1^4}{K_1 + p_1^4}$	$E B(E, S)$	1 3 (17)	Saddle-node
Activation	$\frac{p_2^4}{K_2 + p_2^4}$	Repression	$\frac{K_1}{K_1 + p_1^4}$	$S O$	1 1 (17)	Hopf
Repression	$\frac{K_2}{K_2 + p_2^4}$	Repression	$\frac{K_1}{K_1 + p_1^4}$	$S B(S_1, S_2)$	1 3 (17)	Pitchfork or saddle-node
Basal + activation	$\gamma_1 + \frac{p_2}{K_2 + p_2}$	Basal + activation	$\gamma_2 + \frac{p_1}{K_1 + p_1}$	S	1 (2)	
Basal + activation	$\gamma_1 + \frac{p_2^2}{K_2 + p_2^2}$	Basal + activation	$\gamma_2 + \frac{p_1^2}{K_1 + p_1^2}$	$S B(S_1, S_2) S$	1 3 1 (5)	Saddle-node saddle-node

Equilibrium points were computed by means of Eq. (14) and the regulatory determinant D (21) was used for stability analysis.

^aThe sequence of states is obtained by increasing (k_1^0, k_2^0) at constant values of the other parameters, states are separated by | and the dynamical patterns are characterized by the following symbols: $E \equiv$ stable fixed point at the origin $\tilde{P}(0, 0)$ corresponding to both genes silenced, $S \equiv$ stable fixed point in the positive quadrant, $\tilde{P}_1 > 0, \tilde{P}_2 > 0$, $B(\tilde{P}_1, \tilde{P}_2) \equiv$ two stable fixed points separated by a saddle and $O \equiv$ limit cycle.

^bNumbers of observed fixed points with $\tilde{P}_1 \geq 0, \tilde{P}_2 \geq 0$ before and after the bifurcations are separated by |, the number in parentheses is the degree of the polynomial derived from Eq. (14). It is tantamount to the maximal number of fixed points.

Table 5
Results of numerical sampling of systems with randomly chosen parameter values^a

Regulation \mathbf{G}_1		Regulation \mathbf{G}_2		Dynamical pattern ^b	Bifurcation type	Frequencies of patterns		
Type	$F_1(p_2)$	Type	$F_2(p_1)$					
Activation	$\frac{p_2^2}{\kappa_{21} + \kappa_{22}p_2 + p_2^2}$	2	Repression	$\frac{\kappa_{11}}{\kappa_{11} + \kappa_{12}p_1 + p_1^2}$	0/2	S	1	
Activation	$\frac{p_2^2}{\kappa_{21} + \kappa_{22}p_2 + p_2^2}$	2	Intermediate	$\frac{\kappa_{12}p_1}{\kappa_{11} + \kappa_{12}p_1 + p_1^2}$	1/2	$E B(E, S)$	Saddle-node	0.603 0.397
Activation	$\frac{p_2^2}{\kappa_{21} + \kappa_{22}p_2 + p_2^2}$	2	Activation	$\frac{p_1^2}{\kappa_{11} + \kappa_{12}p_1 + p_1^2}$	2/2	$E B(E, S)$	Saddle-node	0.663 0.337
Activation	$\frac{p_2^2}{\kappa_{21} + \kappa_{22}p_2 + p_2^2}$	3	Repression	$\frac{\kappa_{11}}{\kappa_{11} + \kappa_{12}p_1 + \kappa_{13}p_1^2 + p_1^3}$	0/3	S O	Hopf	0.998 0.002
Activation	$\frac{p_2^3}{\kappa_{21} + \kappa_{22}p_2 + \kappa_{23}p_2^2 + p_2^3}$	3	Intermediate	$\frac{\kappa_{12}p_1}{\kappa_{11} + \kappa_{12}p_1 + \kappa_{13}p_1^2 + p_1^3}$	1/3	$E B(E, S) O$	Saddle-node Hopf	0.642 0.354 0.004
Activation	$\frac{p_2^3}{\kappa_{21} + \kappa_{22}p_2 + \kappa_{23}p_2^2 + p_2^3}$	3	Intermediate	$\frac{\kappa_{13}p_1^2}{\kappa_{11} + \kappa_{12}p_1 + \kappa_{13}p_1^2 + p_1^3}$	2/3	$E B(E, S) O$	Saddle-node Hopf	0.715 0.283 0.002
Activation	$\frac{p_2^3}{\kappa_{21} + \kappa_{22}p_2 + \kappa_{23}p_2^2 + p_2^3}$	3	Activation	$\frac{p_1^3}{\kappa_{11} + \kappa_{12}p_1 + \kappa_{13}p_1^2 + p_1^3}$	3/3	$E B(E, S)$	Saddle-node	0.720 0.280
Activation	$\frac{p_2^4}{\kappa_{21} + \kappa_{22}p_2 + \kappa_{23}p_2^2 + p_2^4}$	4	Repression	$\frac{\kappa_{11}}{\kappa_{11} + \kappa_{12}p_1 + \kappa_{13}p_1^2 + \kappa_{14}p_1^3 + p_1^4}$	0/4	S O	Hopf	0.988 0.012
Activation	$\frac{p_2^4}{\kappa_{21} + \kappa_{22}p_2 + \kappa_{23}p_2^2 + \kappa_{24}p_2^3 + p_2^4}$	4	Intermediate	$\frac{\kappa_{12}p_1}{\kappa_{11} + \kappa_{12}p_1 + \kappa_{13}p_1^2 + \kappa_{14}p_1^3 + p_1^4}$	1/4	$E B(E, S) O$	Saddle-node Hopf	0.673 0.321 0.006
Activation	$\frac{p_2^4}{\kappa_{21} + \kappa_{22}p_2 + \kappa_{23}p_2^2 + \kappa_{24}p_2^3 + p_2^4}$	4	Intermediate	$\frac{\kappa_{13}p_1^2}{\kappa_{11} + \kappa_{12}p_1 + \kappa_{13}p_1^2 + \kappa_{14}p_1^3 + p_1^4}$	2/4	$E B(E, S) O$	Saddle-node Hopf	0.740 0.258 0.002
Activation	$\frac{p_2^4}{\kappa_{21} + \kappa_{22}p_2 + \kappa_{23}p_2^2 + \kappa_{24}p_2^3 + p_2^4}$	4	Intermediate	$\frac{\kappa_{14}p_1^3}{\kappa_{11} + \kappa_{12}p_1 + \kappa_{13}p_1^2 + \kappa_{14}p_1^3 + p_1^4}$	3/4	$E B(E, S)$	Saddle-node	0.751 0.249
Activation	$\frac{p_2^4}{\kappa_{21} + \kappa_{22}p_2 + \kappa_{23}p_2^2 + \kappa_{24}p_2^3 + p_2^4}$	4	Activation	$\frac{p_1^4}{\kappa_{11} + \kappa_{12}p_1 + \kappa_{13}p_1^2 + \kappa_{14}p_1^3 + p_1^4}$	4/4	$E B(E, S)$	Saddle-node	0.742 0.258

^aThe frequencies of bifurcation patterns are derived from a large number ($N > 10\,000$) of randomly chosen combinations of parameters. The values for a parameter π are taken from the interval $-9.25 \leq \log \pi \leq 9.25$ under the assumption of a uniform distribution of $\log \pi$ (see also Section 5).

^bThe sequence of states is obtained by increasing (k_1^Q, k_2^Q) at constant values of the other parameters, states are separated by | and the dynamical patterns are characterized by the symbols described in the footnote of Table 4.

every gene. The stationary protein concentrations are obtained as solutions of polynomials. Since the polynomials are of high degrees for cooperative systems (Hill coefficient $n \geq 2$) a combined analytical and computational technique, consisting of the numerical calculation of the polynomial roots, is mandatory. Despite high degrees the polynomials allow for an analytical handling of limits like high and low binding affinities. Local stability analysis is performed in terms of the eigenvalues of the Jacobian matrix at fixed points.

In this contribution we presented examples for a (quite general) class of genetic regulations—denoted here as *simple*—where the analysis of the Jacobian is largely facilitated by its structure (21): computation of the regulatory determinant D is sufficient for the stability analysis of fixed points. At two computable critical values, D_{OneD} and D_{Hopf} , the fixed points become unstable through a one-dimensional bifurcation or a Hopf bifurcation, respectively. Fixed points are stable in between, $D_{\text{OneD}} < D < D_{\text{Hopf}}$. It is important for generalizations that D_{OneD} is always negative whereas D_{Hopf} always has positive sign. For two-gene systems the class *simple* is constituted by cross-catalysis which expresses that regulatory binding functions depend only on the concentration of the protein derived from the other gene: $F_1(p_2)$ and $F_2(p_1)$. Apart from this restriction the binding functions can be arbitrarily complicated, only differentiability is required for the computation of D : examples for more complicated cases analyzed here are leaky transcription (two terms) and intermediate complexes as transcription initiators.

The approach can be readily extended to more than two genes and there the properties of the class *simple* are fulfilled by catalytic cycles consisting of a closed loop of regulatory functions, $\mathbf{G}_N \Rightarrow \mathbf{G}_1 \Rightarrow \mathbf{G}_2 \Rightarrow \dots \Rightarrow \mathbf{G}_N$ for arbitrary N . A description of such regulatory systems by means of dynamical graphs has been reported in Remy et al. (2003). One concrete example of a regulatory loop with $N = 3$ is the repressilator Elowitz and Leibler (2000) which has been analyzed in detail (for example, in Müller et al., 2006). On the other hand, there are also examples of two-gene systems that do not fall under the classification *simple*, for example, self-activation and cross-repression or self-repression and cross-activation, because then the regulatory binding functions depend on the concentrations of both proteins: $F_1(p_1, p_2)$ and $F_2(p_1, p_2)$. Attempts to generalize our approach and to group these *non-simple* systems into subgroups according to the dynamical structure related to the difficulty of analysis are under way (Schuster et al., 2006).

The dynamical pattern of gene regulation has been analyzed for several cooperative binding functions, $F_1(p_2)$ and $F_2(p_1)$, with different Hill coefficients by means of a new technique using the regulatory determinant $D(p_1, p_2)$ introduced and defined in Eq. (21). We computed and classified only the generic dynamic features and the bifurcation patterns which were found in full agreement with the literature wherever results from previous studies

were available. No attempt has been made yet to make a complete search in parameter space, nor did we try in this paper to adjust to experimental data. Therefore, concentrations and parameter values were chosen to illustrate best the basic features of the bifurcation diagrams and the oscillatory dynamics. A forthcoming study will deal with fitting regulatory dynamics to experimental data by making use of inverse methods (Engl et al., 1996; Woodbury, 2002). A particularly challenging problem is reverse engineering of bifurcation patterns, first approaches to this problem are now available (Lu et al., 2006).

All cooperative systems (except activation–repression with Hill coefficient $n = 2$) show an unregulated and a regulated regime. The regulated regime is reached at sufficiently high values of the ratio ϑ/K implying that: (i) transcription and translation are fast enough compared to mRNA and protein degradation and (ii) binding is sufficiently strong. The *pure* systems¹¹ fall into three classes: **act–act**, **act–rep**, and **rep–rep**. Each class has its own regulatory characteristic: (i) **act–act** leads to both genes active or both genes silenced, (ii) **act–rep** results in oscillatory activity of the two genes and (iii) **rep–rep** represents a bistable switch with the two states: (i) \mathbf{G}_1 active and \mathbf{G}_2 silenced and vice versa, (ii) \mathbf{G}_1 silenced and \mathbf{G}_2 active. In pure systems D is either always negative (**act–act** and **rep–rep**) or always positive (**act–rep**) and accordingly we find bistability only in the first two classes of systems and oscillations occur exclusively in the third class. More complicated binding functions may give rise to mixed behavior resulting from simultaneous appearance of one-dimensional and Hopf bifurcations in the same bifurcation diagram. The cases of intermediate regulation discussed in Section 4.5 may serve as examples.

The model for gene regulation and the technique for analyzing regulatory dynamics presented here provides a fast tool for computational bifurcation analysis. The parameter spaces of small genetic networks with several genes can be scanned completely. Regulatory systems can be classified into *simple* and *non-simple* systems according to the structure of the Jacobian matrix. *Simple* systems are accessible to a highly efficient combined analytical and computational approach. Analytical expressions are available for the computation of bifurcation points. The current procedure will be developed further into an automatic tool for the exploration of entire parameter spaces that is applicable to systems with several genes (up to approximately five genes). Future work aims also at an up-scaling to systems with many genes.

Acknowledgments

This work has been supported financially by the Austrian ‘Fonds zur Förderung der wissenschaftlichen

¹¹The term *pure* indicates that the complex active in transcription is either fully saturated— $\mathbf{H}^{(4)}$ in Fig. 15 implying activation (**act**)—or unbound— \mathbf{G} in Fig. 15 indicating repression (**rep**).

Forschung' (FWF, Projects: P-13887 and P-14898). It is also part of the project on 'Inverse Methods in Biology and Chemistry' sponsored by the 'Wiener Wissenschafts-, Forschungs- und Technologiefonds' (WWTF, Project: MA05). Part of the work has been carried out during a visit at the Santa Fe Institute within the External Faculty Program. All support as well as fruitful discussions with Professors Heinz Engl, Josef Hofbauer and Karl Sigmund, Drs. Christoph Flamm, James Lu and Stefan Müller and Mag. Lukas Endler are gratefully acknowledged.

Appendix A. Condition for a Hopf bifurcation

In order to compute the value \bar{D}_{Hopf} (Fig. 2) where the two-gene system loses stability at positive values of D , we use the criterion by Liénard–Chipart (see Gantmacher, 1998, p. 221). According to that criterion, the eigenvalues of the Jacobian have strictly negative part if and only if the zeroth, second and fourth coefficient of the secular equation as well as the second and fourth Hurwitz determinant are positive. The latter two are determinants of 2×2 and 4×4 matrices, respectively, whose non-zero entries are coefficients of the secular equation.

From Eq. (21), the zeroth and the second coefficient are always positive, and the fourth coefficient is positive for $D > -d_1^Q d_2^Q d_1^P d_2^P$. The second Hurwitz determinant is always positive because it expands to an expression in $d_1^Q, d_2^Q, d_1^P, d_2^P$ with positive coefficients. The fourth Hurwitz determinant is a quadratic polynomial in D . With the help of the computer algebra system Maple, one finds that it has two real roots, corresponding to the values

$$D_{\text{trans}} = -d_1^Q d_2^Q d_1^P d_2^P \quad \text{and} \quad (22)$$

$$\bar{D}_{\text{Hopf}} = \frac{(d_1^Q + d_2^Q)(d_1^Q + d_1^P)(d_1^Q + d_2^Q)(d_2^Q + d_1^P)(d_2^Q + d_2^P)(d_1^P + d_2^P)}{(d_1^Q + d_2^Q + d_1^P + d_2^P)^2}. \quad (24)$$

Between these two roots it is positive because its leading coefficient is negative, the eigenvalues of the Jacobian have strictly negative real parts and the corresponding fixed point is asymptotically stable.

References

- Albert, R., Othmer, H.G., 2003. The topology of the regulatory interactions predicts the expression pattern of the segment polarity genes in *Drosophila melanogaster*. *J. Theor. Biol.* 223, 1–18.
- Biebricher, C.K., Eigen, M., 1987. Kinetics of RNA replication by $Q\beta$ replicase. In: Domingo, E., Holland, J.J., Ahlquist, e.P. (Eds.), *RNA Genetics I: RNA-Directed Virus Replication*. Plenum Publishing Corporation, Boca Raton, FL, pp. 1–21.
- Biebricher, C.K., Eigen, M., Gardiner Jr., W.C., 1983. Kinetics of RNA replication. *Biochemistry* 22, 2544–2559.
- Bindschadler, M., Sneyd, J., 2001. A bifurcation analysis of two coupled calcium oscillators. *Chaos* 11, 237–246.
- Cantor, C.R., Schimmel, P.R., 1980. *Biophysical Chemistry*, vols. I–III. W.H. Freeman, San Francisco, CA.
- Cherry, J.L., Adler, F.R., 2000. How to make a biological switch. *J. Theor. Biol.* 203, 117–133.
- Craciun, G., Tang, Y., Feinberg, M., 2006. Understanding bistability in complex enzyme-driven reaction networks. *Proc. Natl Acad. Sci. USA* 103, 8697–8702.
- Elowitz, M.B., Leibler, S., 2000. A synthetic oscillatory network of transcriptional regulators. *Nature* 403, 335–338.
- Engl, H.W., Hanke, M., Neubauer, A., 1996. *Regularization of Inverse Problems—Mathematics and its Applications*. Springer, Berlin.
- Ferrell, J.E., 2002. Self-perpetuating states in signal transduction: positive feedback double feedback and bistability. *Curr. Opin. Cell Biol.* 14, 140–148.
- Gantmacher, F.R., 1998. *The Theory of Matrices*, vol. 2. AMS Chelsea Publishing, Providence, RI. Reprint of the 1959 Translation from Russian by K.A. Hirsch.
- Gardner, T.S., Cantor, C.R., Collins, J.J., 2000. Construction of a genetic toggle switch in *Escherichia coli*. *Nature* 403, 339–342.
- Goodwin, B.C., 1965. Oscillatory behavior in enzymatic control processes. *Adv. Enzyme Regul.* 3, 425–439.
- Guet, C.C., Elowitz, M.B., Hsing, W., Leibler, S., 2002. Combinatorial synthesis of genetic networks. *Science* 296, 1466–1470.
- Hartwell, L.H., Hopfield, J.J., Leibler, S., Murray, A.W., 1999. From molecular to cellular biology. *Nature* 402 (Suppl.), C47–C52.
- Hill, A.V., 1910. The possible effects of the aggregation of the molecules of haemoglobin on its dissociation curve. *J. Physiol.* 40 (Section 11.2.1), iv–vii.
- Hume, D.A., 2000. Probability in transcriptional regulation and its implications for leukocyte differentiation and inducible gene expression. *Blood* 96, 2323–2328.
- Jacob, F., Monod, J., 1961. Genetic regulatory mechanisms in the synthesis of proteins. *J. Mol. Biol.* 3, 318–356.
- Kobayashi, T., Chen, L., Aihara, K., 2003. Modeling genetic switches with positive feedback loops. *J. Theor. Biol.* 221, 379–399.
- Kovacs, I., Silver, D.S., Williams, S.G., 1999. Determinants of commuting-block matrices. *Am. Math. Mon.* 106, 950–952.
- Lu, J., Engl, H.W., Schuster, P., 2006. Inverse bifurcation analysis: application to simple gene systems. *Algorithms Mol. Biol.* 1, 11.
- Marcus, M., 1987. Two determinant condensation formulas. *Linear Multilinear Algebra* 22, 95–102.
- Monod, J., Changeaux, J.-P., Jacob, F., 1963. Allosteric proteins and cellular control systems. *J. Mol. Biol.* 6, 306–329.
- Müller, S., Hofbauer, J., Endler, L., Flamm, C., Widder, S., Schuster, P., 2006. A generalized model of the repressor. *J. Math. Biol.* 53, 12–14.
- Ptashne, M., Gann, A., 2002. *Genes & Signals*. Cold Spring Harbor Laboratory Press, Cold Spring Harbor, NY.
- Remy, E., Mossé, B., Chouïya, C., Thieffry, D., 2003. A description of dynamical graphs associated to elementary regulatory circuits. *Bioinformatics* 19 (Suppl. 2), ii172–ii178.
- Savageau, M.A., 2001. Design principles for elementary gene circuits: elements, methods and examples. *Chaos* 11, 142–159.
- Schuster, P., 2005. Binding of activators and repressors to DNA. Part I: equilibria. Working Paper 05-05-016, Santa Fe Institute, Santa Fe, NM.
- Schuster, P., Flamm, C., Endler, L., 2006. Dynamic patterns of gene regulation II: double regulatory functions and many gene interactions. Working paper, University of Vienna, Vienna, Austria.
- Smith, H., 1987. Oscillations and multiple steady states in a cyclic gene model with repression. *J. Math. Biol.* 25, 169–190.
- Thattai, M., Shraiman, B.I., 2003. Metabolic switching in the sugar phosphotransferase system of *Escherichia coli*. *Biophys. J.* 85, 744–754.
- Thomas, R., D'Ari, R., 1990. *Biological Feedback*. CRC Press, Boca Raton, FL.
- Thomas, R., Kaufman, M., 2001a. Multistationarity, the basis of cell differentiation and memory. II. Logical analysis of regulatory networks in terms of feedback circuits. *Chaos* 11, 170–179.

- Thomas, R., Kaufman, M., 2001b. Multistationarity, the basis of cell differentiation and memory. II. Structural conditions of multistationarity and other nontrivial behavior. *Chaos* 11, 180–195.
- Tiwari, J., Fraser, A., Beckmann, R., 1974. Genetic feedback repression. I. Single locus models. *J. Theor. Biol.* 45, 311–326.
- Tyson, J.J., Othmer, H.G., 1978. The dynamics of feedback control circuits in biochemical pathways. *Prog. Theor. Biol.* 5, 1–62.
- Tyson, J.J., Chen, K.C., Novak, B., 2003. Sniffers, buzzers, toggles and blinkers: dynamics of regulatory and signalling pathways in the cell. *Curr. Opin. Cell Biol.* 15, 221–231.
- Woodbury, K.A. (Ed.), 2002. *Inverse Engineering Handbook*. CRC Press, Boca Raton, FL.
- Yokobayashi, Y., Weiss, R., Arnold, F.H., 2002. Directed evolution of a genetic circuit. *Proc. Natl Acad. Sci.* 99, 16587–16591.